PRODUCTION OF HOLLOW FIBERS BY CO-ELECTROSPINNING OF CELLULOSE ACETATE

by

Abdurizzagh Khalf

Thesis submitted in partial fulfilment
of the requirements for the degree

of

MASTER OF SCIENCE IN ENGINEERING
(CHEMICAL ENGINEERING)

In the Department of Process Engineering
at the University of Stellenbosch

Study Leaders

Prof JH Knoetze

Prof RD Sanderson

March 2009

Declaration

I, the undersigned, hereby declare that the work contained in this thesis is my own original work and that I have not previously in its entirety or in part submitted it at any university for a degree.

…… …….. …….

Signature Date

March 2009

ABSTRACT

Production of hollow fibers by co-electrospinning of cellulose Acetate

---

The study concerns the use of the electrospinning technique for the formation of cellulose acetate hollow nanofibers. These hollow fibers are used to manufacture hollow fiber membranes. Important properties that should be inherent to these hollow-nanofibers include excellent permeability and separation characteristics, and long useful life. They have potential applications in filtration, reverse osmosis, and the separation of liquids and gases.

It is apparent from the available literature on electrospinning and co-electrospinning that the diameter and the morphology of the resulting fibers are significantly influenced by variations in the system and process parameters, which include the solution concentration, solvent volatility, solution viscosity, surface tension and the conductivity of the spinning solution.

The materials used include cellulose acetate (CA) (concentration = 11~14 wt %), (feed rate = 1~3 ml/h), acetone:dioxane (2:1) and mineral oil (feed rate = 0.5~1 ml/h) with core and shell linear velocity of 2 and 0.7 mm/min respectively. These materials were used as received without further purification.

The co-electrospinning setup used comprised a compound spinneret, consisting of two concentric small-diameter capillary tubes/needles, one located inside another (core-shell/co-axial design). The internal and external diameters of the inside and outside needles were 0.3 and 1.2 mm respectively (0.3 mm shell/core gap space). The liquids CA (shell) and mineral oil (core) are pumped to the coaxial needle by a syringe pump, forming a compound droplet at the tip of the needle. A high voltage source is used to apply a potential of several kilovolts over the electrospinning distance. One electrode is placed into the spinning solution and the other oppositely charged (or neutral) electrode attached to a conductive collector. If the charge build up reaches approximately 15 kV the charged compound droplet, (poorly conductive polymer solution) deforms into a conical structure called a Taylor cone. On further increasing, the charge at the Taylor cone to some critical value (unique to each polymer system) the surface tension of the compound Taylor cone is broken and a

core-shell jet of polymer solution ejects from the apex of the Taylor cone. This jet is linear over a small distance, and then deviates in a course of violent whipping from bending instabilities brought about by repulsive charges existing along the jet length. The core-shell jet is stretched and solvent is evaporated and expelled, resulting in the thinning and alignment of the fiber. Ultimately dry (most solvent having been removed) submicron fibers are collected in alignment form in a simple collector design (water bath).

The shell to core solution flow rate ratio was chosen according to the parameter response of shell-core diameter of the resulting fibers in order to achieve an optimal hollow structure after removal of the mineral oil core. The mineral oil of the dry collected core-shell fibers is removed by immersion in octane. The aforementioned response is determined by measurement of core-shell diameters using scanning electron microscopy (SEM) and transmission electron microscopy (TEM).

The obtained results showed that the ability of the spinning solution to be electrospun was directly dependent on its concentration and the feed rate of the spinning solution and also parameters such as the spinning distance and type of solvents used. The preferable polymer solution concentration is 14 wt %, shell feed rate of 3 ml/hr, core feed rate of 0.5 ml/hr (2 and 0.7 mm/s core and shell linear velocity respectively), applied voltage of 15 KV, spinning distance of 8 cm and coaxial spinnerets having internal diameters of 0.3 mm and 1.2 mm core and shell needles respectively (0.3 mm shell/core gap space) have been found to make uniform cellulose acetate hollow fibers with an average inside and outside diameter of approximately 495 and 1266 nm, respectively.

Opsomming

Vervaardiging van holvesels deur gelyktydige elektrospinnery van selluloseasetaat

---

Hierdie studie handel oor die gebruik van die elektrospin-tegniek vir die vervaardiging van selluloseasetaat-holnanovesels. Hierdie holvesels word gebruik om holvesel-membrane te vervaardig. Belangrike eienskappe wat onafskeidelik aan hierdie holnanovesels verbonde behoort te wees, sluit uitstekende permeabiliteit en skeidingseienskappe, asook ’n lang, nuttige lewensduur in. Hierdie eienskappe kan moontlik in filtrering, tru-osmose en die skeiding van vloeistowwe en gasse toegepas word. Uit die beskikbare literatuur oor elektrospinnery en gelyktydige elektrospinnery is dit duidelik dat die diameter en die morfologie van die elektrogespinde vesels aanmerklik beïnvloed word deur variasies in die stelsel en prosesparameters, wat die spinoplossingkonsentrasie, viskositeit, oplossingsverande-rlikheid, oppervlakspanning en geleidingsvermoë van die spinoplossing insluit.

Die volgende materiale is gebruik: selluloseasetaat (CA) (konsentrasie 11~14 gew. %, voertempo 1~3 ml/u), asetoon:dioksaan (2:1) en mineraalolie (voertempo 0.5~1 ml/u), kern- en skil- lineêre snelheid 2 en 0.7 mm/min onderskeidelik.

Die gelyktydige elektrospin-stelsel wat gebruik is, het ’n saamgestelde spindop bevat, wat uit twee konsentriese klein-diameter-haarbuise/-naalde, een binne die ander (kern-skil-/koaksiale ontwerp), bestaan. Die interne en eksterne diameters van die binneste en buitenste naalde was 0.3 en 1.2 mm onderskeidelik (0.3 mm skil/kern-gapingspasie). Die vloeistowwe SA (skil) en mineraalolie (kern) is in die koaksiale naald met behulp van ’n spuitpomp gepomp, wat ’n saamgestelde druppeltjie aan die punt van die naald gevorm het. ’n Hoëspanningsbron is gebruik om ’n moontlikheid van verskeie kilovolts oor die elektrospin-afstand toe te pas. Een elektrode is in die spinoplossing geplaas, en die ander teenoorgesteld gelaaide (of neutrale) elektrode is aan ’n geleidende kollektor geheg. As die opgeboude lading ongeveer 15 kV bereik, vervorm die gelaaide saamgestelde druppeltjie (swak geleidende polimeeroplossing) tot ’n kegelvormige struktuur genaamd ’n Taylor-keël. Met verdere verhoging van die lading op die Taylor-keël tot ’n kritieke waarde (eie aan elke polimeerstelsel) word die oppervlakspanning van die saamgestelde

Taylor-keël verbreek en spuit ’n kern-skil-straal polimeeroplossing uit die toppunt van die Taylor-keël. Hierdie straal is lineêr oor ’n kort afstand, en wyk dan af in ’n reeks heftige opwippings weens buiginstabiliteite wat deur terugstotende ladings met die lengte van die straal langs veroorsaak word. Die kern-skil-straal word gestrek en die oplossing evaporeer en word uitgeskei, wat tot die verdunning en inlynstelling van die vesel lei. Uiteindelik word droë (die meeste van die oplossing is verwyder) submikronvesels in lynstellingsvorm in ’n eenvoudige, kollektorontwerp (waterbad) versamel.

Die verhouding van die skil-tot-kern-oplossingsvloeitempo is volgens die parameterreaksie van die skil-kern-diameter van die voortspruitende vesels gekies ten einde ’n optimale holstruktuur ná verwydering van die mineraalolie-kern te verkry. Die mineraalolie van die droë versamelde kern-skilvesels is deur indompeling in oktaan verwyder. Die genoemde reaksie is deur meting van die kern-skil-diameters met behulp van skandeer-elektronmikroskopie (SEM) en transmissie-elektronmikroskopie (TEM) bepaal.

Die resultate het getoon dat die vermoë van die spinoplossing om elektrogespin te word, direk afhanklik was van die konsentrasie en die voertempo van die spinoplossing, asook van parameters soos die spinafstand en soort oplossings wat gebruik is. Die voorkeur-polimeeroplossingskonsentrasie is 14 gew. %, skil-voertempo van 3 ml/u, kern-voertempo van 0.5 ml/u (2 en 0.7 mm/s kern- en skil-lineêre snelheid onderskeidelik). Daar is gevind dat toegepaste spanning van 15 kV, spinafstand van 8 cm en koaksiale spindoppe met interne diameters van 0.3 mm en 1.2 mm kern- en skilnaalde onderskeidelik (0.3 mm skil-/kern-gapingspasie) eenvormige selluloseasetaat-holvesels met ’n gemiddelde binne- en buitediameter van ongeveer 495 en 1 266 nm onderskeidelik vervaardig.

TABLE OF CONTENTS

List of Abbreviations and Symbols

CA	cellulose acetate
Conc	concentration (g/ml)
D	fibre diameter (nm)
DF	degree of freedom
DMAc	dimethylacetamide
DSC	differential scanning calorimetry
E	applied voltage (kV)
Eu	Euler number
GPC	Gel Permeated Chromatography
hr	hour
h_t	final jet diameter (m)
I	electric current (Coulomb/s)
ID	inner fiber diameter (nm)
k	conductivity of the fluid (μS/cm)
kV	kilovolts
Level	typically factor levels (+1,-1)
MF	microfiltration
min	minutes
M_n	average molecular number
M_w	average molecular weight
M_z	z-average molecular weight
NF	nanofiltration
OD	outer fiber diameter (nm)
Prop>F	probability of seeing the observed F value

Q	flow rate (kg/s)
R	dimensionless jet radius
r	radius of the jet (m)
Re	Reynolds number
SEM	scanning electron microscopy
SS	sum of squares
SSt	total sum of squares
t	time
T	temperature (^{o}C)
T_g	glass transition temperature (^{o}C)
u	velocity (m/s)
UF	ultrafiltration
v/v	volume ratio of solvent
We	Weber number
z	displacement of the centreline of the jet (μm)
γ	surface tension (N/m)
δ	Shear rate (1/s)
Δ	difference
η	solution viscosity (in poise)
ρ	liquid density (g/ml)
σ	surface density of the charge (Coulomb/m^2)
Є	dielectric permittivity

Acknowledgments

First, I would like to thank Allah, for giving me strength and hope to complete this work. I thank my study leaders, Prof Knoetze and Prof Sanderson for giving me the opportunity to work under their guidance. I would also like to thank Dr Goldie for his contribution to the success of my research. Thanks to my parents, for their love and support throughout my life. Thank you to all my family that have supported and encouraged me.

I would also like to thank the following people/departments:

Haydn, Margie, Ulrich, Eugene, Deon, Aneli and Erinda;

North South Africa Technologies (NSAT);

Central Analytical Facility (SEM unit), University of Stellenbosch;

Electron Microscopy Unit, University of Cape Town;

Physics Department workshop, University of Stellenbosch

List of Tables

Appendix

List of Figures

Appendix

Chapter 1

Introduction and objectives

1.1 Introduction

Electrospinning is a unique technique for the production of submicron fibers through an electrically charged jet of polymer solution. In electrospinning, fibers with diameters smaller than 1000 nm are named nanofibers [1]. Nanofibers are solid state, linear continuous nanomaterials possessing a very large area per volume ratio. These properties made them very attractive in a wide range of applications such as in filtration media, tissue engineering, protective clothing, membranes in affinity separation [2, 3] and sound dampening.

Electrospun nanofiber membranes possess several attractive attributes that make them very useful in separation technology [3], and they have three major advantages: low-cost operation, energy-efficiency, a high surface area and a high rate of adsorption [3]. Microfiltration (MF) is an important separation operation for membrane pretreatment, and water and air purification [4]. Most of the commercial microfiltration media are inherently non-homogeneous in mass and thickness. Good permeability and filtration performance, and a uniform structure, are important objectives during the fabrication of MF membranes [4].

Asymmetric cellulose acetate (CA) membranes are widely used for reverse osmosis (RO), (MF) and gas separation. CA membranes offer high performance and good chlorine resistance [4]. The hollow fibers membrane configuration has become a favourite choice for the following reasons: (a) hollow fibers are self-supporting, meaning they can be backwashed to recover the flux, (b) hollow fibers have a much larger ratio of membrane area to unit volume compared to flat and spiral-wound membranes, (c) hollow fiber membrane have good flexibility in the mode of operation [5].

Co-electrospinning is a modern technique of electrospinning that can be used to produce hollow fibers by using a coaxial capillary consisting of two concentric needles located one inside another. Many different polymers have been electrospun into core-shell fibers using two immiscible polymers (this is covered in detail in chapter 2, section 2.7, Table 2.3). Several research groups* have proved that hollow nanofibers can be fabricated by co-electrospinning of both miscible and immiscible polymer solutions.

*Jiang et al. 2005 [25], Wang et al. 2006 [45]and Li et al. 2004 [49]

1.2 Objectives and scope of this study

Electrospinning is a relatively simple technique that can be used to produce nanofibers using an electrostatic force. The fibers obtained in this process are solid and are randomly oriented. Some important applications for these nanofibers include, sound dampening, wound dressing, filtration, catalytic substrates, and cell scaffolding. However, conventionally produced hollow fiber membranes have found wide spread application in filtration. Preparation of nanofibers in a core-shell configuration, using two dissimilar solutions, via a novel technique of co-electrospinning has presented the capability to electrospin polymer solutions that meet the essential requirements for core-shell fibers. Therefore, this study aims to use electrospinning technology in the fabrication of CA ollow fibers. This involves the following:

1. Fabrication of CA hollow fiber by co-electrospinning:
    a) Design suitable coaxial needle
    b) Production of core-shell fibers
    c) Alignment of electrospun core-shell fibers
    d) Extract the cores to form hollow fibers
2. Statistical analysis to study the effect of the electrospinning process and the system parameters on the response variables (core and shell diameter) and the interaction effect between the factors.
3. Determine the preferable conditions for production of hollow fibers by co-electrospinning of CA.

1.3 Hypothesis

For both the electrospinning and co-electrospinning processes the structure and morphology of the final products are significantly influenced by the various system parameters and process parameters. It is therefore assumed that in electrospinning of the core-shell polymer fibers the solution properties, including the polymer molecular weight, solution concentration, solvent volatility, solution viscosity, surface tension, and conductivity of the solution will strongly affect the morphology and the diameter of the resulting fibers.

1.4 Layout of thesis

This study of the production of hollow fibers by co-electrospinning of cellulose acetate consists of six chapters.

Chapter 1 introduces the topic and the objectives including scope of the work.

Chapter 2 gives a theoretical background on electrospinning and co-electrospinning, their processing approaches, and the process and system of electrospinning parameters.

Chapter 3 describes the materials used and the experimental methods used for the electrospinning of CA/oil, aligning of CA core-shell fibers and characterizing the resulting fibers. Scanning electron microscopy, transmission electron microscopy, and fiber diameter measurement via image analysis were used for the characterization.

Chapter 4 presents the design validation and the results of the experiments and discussion of the effect of the electrospinning parameters on the behaviour of the jet and the specific parameters of CA electrospun fibers.

Chapter 5 describes factorial design experiments that were used to investigate the factors that have a major effect on the electrospun fibers and what interaction there may be between factors.

Chapter 6 gives conclusions for this study and recommendations for future work.

Appendix includes supportive data, tables of properties and SEM images.

Chapter 2

Theoretical background and literature review

2.1 Conventional spinning

Spinning has long been known as the method for the production of fibers on a commercial scale. The world is currently consuming enormous quantities of these fibers in the form of clothing, carpets, furniture upholstery, etc., and the demand is expected to increase even further in the future [6]. There are three important types of spinning processes:

2.1.1 Melt spinning

In melt spinning the raw polymer material is melted by heating it to high temperature (higher than the melting temperature) and the material is then extruded through a spinneret. Melt spun fibers can be extruded from the spinneret (Figure 2.1) in various cross-sectional forms (trilobal, round, pentagonal, octagonal) [6].

2.1.2 Dry spinning

The mechanism of producing fibers by dry spinning is directly dependent on evaporation of polymer solvent. The polymer solution is extruded through a spinneret into a heated zone where the solvent evaporates, leaving behind fiber filaments [6].

2.1.3 Wet spinning

In wet spinning the polymer–non-volatile solvent mixture is extruded through spinnerets. The spinnerets are totally submerged in a non-solvent coagulate solution. As the filaments emerge, they precipitate from solution, and solidify [6].

Conventional spinning methods cannot produce woven or non-woven fibers with diameters small as 100 nm. The technique that has the ability to produce fibers of the order of 100 nm is known as electrospinning [6, 7].

Figure 2.1: Fibers produced from a melt spinning machine [7].

2.2 Electrospinning

In 1934, a process was patented by Formhals [8] for the production of polymer filaments using electrostatic force: the process is known as electrospinning (see Figure 2.2) Formhals electrospun CA fibers by using a spinning solution of CA in ethylene glycol. His method involved dispersing the spinning solution using a high voltage source (Figure 2.2). One of the disadvantages of his device was the difficulty in transferring the electrospun fibers that stuck to the collector belt [8, 9].

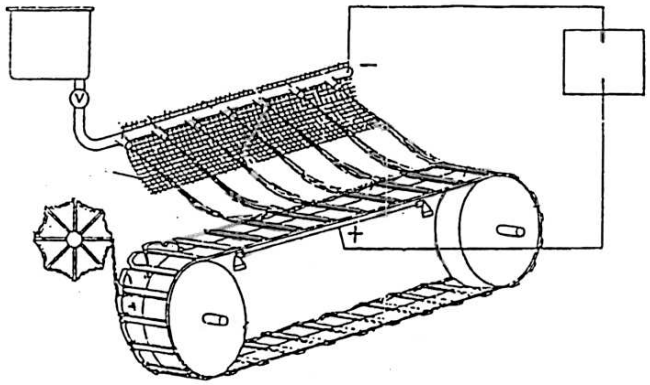

Figure 2.2: Schematic of Formhals electrospinning design [8].

2.2.1 Definition

Electrospinning is a process in which sub-micron polymer particles, fibers or interconnected porous fiber meshes can be produced using an electrostatically driven jet of polymer solution. Electrospinning is able to produce continuous fibers with submicron diameters and diameters down to the nanometer diameter range. These fibers have a large surface area to volume ratio, which significantly increase their absorption efficiency [7]. Progress in electrospinning had reached a plateau by the mid-1990s, when interest was re-gained by the research of Reneker [10], who realized the huge potential of the process for nanofibers production. In the fiber industries, a major consideration is the rate of fiber production. Electrospinning, compared to the popular industrial fiber spinning processes, is very slow. Industrial dry spinning has a yarn take-up rate of 200-1500 m/min, while yarn fabricated by electrospinning has a take-up rate of 30 m/min [11].

2.2.2 Process and setup

The electrospinning setup consists of a high voltage supplier, a syringe pump, a conductive collector plate and a spinneret [12]. The solution is pumped to the needle tip by a syringe pump and forms a compound droplet at the tip of the needle. A high voltage source is used to apply a potential of several kilovolts over the electrospinning distance. One electrode is placed in the spinning solution and the other oppositely charged or neutral electrode attached to a conductive collector [13]. If the charge build-up reaches an order of approximately 10 kV the charged compound droplet deforms into a conical structure called a Taylor cone. The Taylor cone is broken and a jet of polymer solution is ejected. This jet is linear for a small distance and then deviates in a course of violent whipping from bending instabilities. This includes three stages of instability. In the first stage, the polymer ejects from the nozzle and stretches smoothly by electrostatic force, in the second stage bending instability occurs farther downstream when the jet gets sufficiently thin, in the third stage the elongation of the jet is stopped by solidification of a thin jet. Wannatong et al. [14] reported that there are six forces that act and affect the behaviour of the charged jet. These forces are listed in Table 2.1.

Table 2-1: List of forces acting on the jet during the electrospinning process

Force	**Description**
Gravitational	The force applied by gravity on the charged jet.
Electrostatic	The force that carries the charged jet from the spinneret to the target.
Columbic	The force that responsible for the stretching of the charged jet during its flight to the target.
Viscoelastic	The force that tries to prevent the charged jet from stretching.
Surface tension	The force that acts against the stretching of the surface of the charged jet.
Drag	The force that results from the friction between the charged jet and the surrounding air.

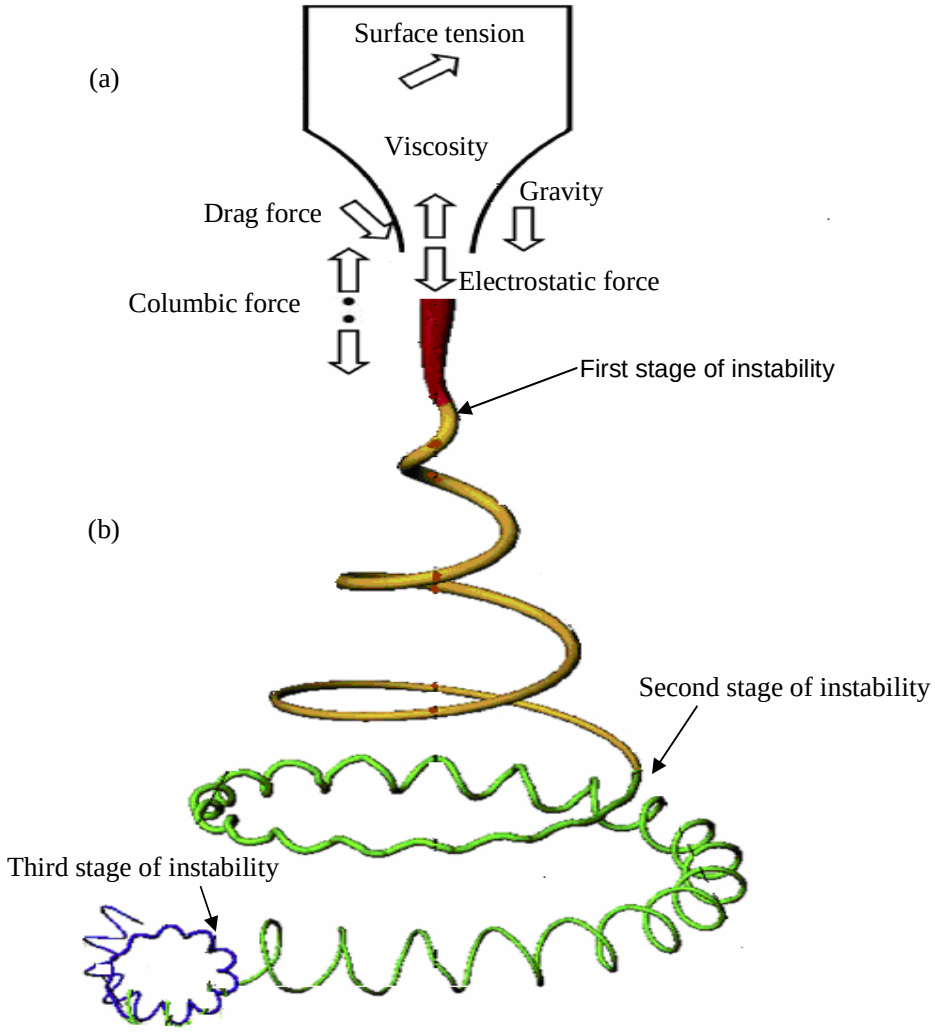

Figure 2.3: (a) Schematic of the forces acting on a droplet at the tip of the needle, and (b) view of the first, second and third stage of whipping instability from a Taylor cone [15].

Figure 2.3 shows a diagram of the forces that act on a droplet at the end of the spinneret. Figure 2.4 shows the basic components required to perform electrospinning.

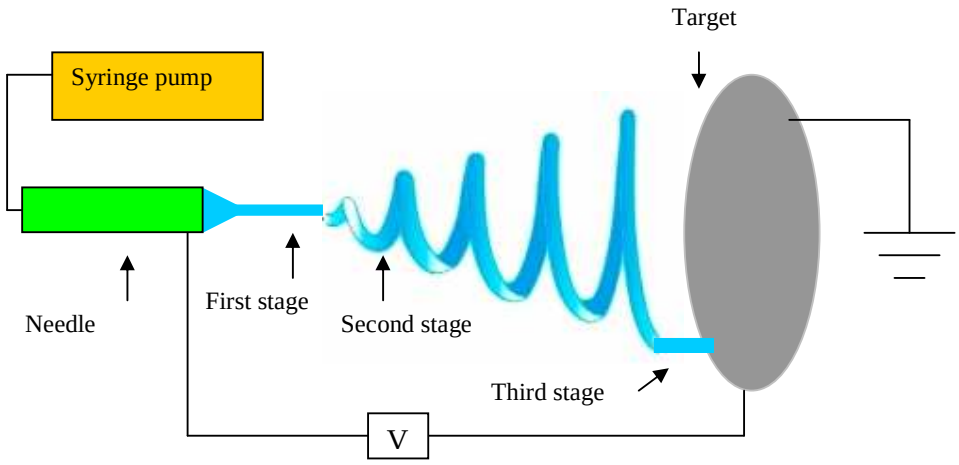

Figure 2.4: Basic components of the electrospinning process.

2.2.3 Features of electrospun nanofibers

An important characteristic of electrospinning is the ability to make fibers with

- diameters ranging from nanometres to a few micrometers,
- high surface area/volume ratio,
- a porous structure,
- a highly ordered structure, and
- a high rate of adsorption, high efficiency of transport, and high strength-to-weight characteristics.

Figure 2.5 shows a photograph of highly ordered nanofibers.

Figure 2.5: Photograph of highly ordered nanofibers.

2.2.4 Polymer properties

Polymers consist of a long chain of molecules with repeating units called monomers that are mostly covalently bonded to one another. The majority of polymers are inexpensive as they have simple elements, and they are relatively easy to synthesize. There are two types of polymers namely thermoplastic and thermo set. In thermoplastics, the linear polymers melt when heat is applied and solidifies when cooled. For thermosetting polymer cross linking between polymer chains occurs when heat is applied. Subsequent application of heat would only degrade the polymer [16].

2.2.4.1 Polymer crystallinity

A polymer is said to be amorphous when the arrangement of the linear molecules is completely random. Polymers that are of higher crystallinity have higher yield strength, modulus and hardens. When crystalline polymers are stretched, the polymer chains are oriented in the direction of the stress and destroy the spherulites structure [16].

2.2.4.2 Polymer molecular weight

Molecular weight of the polymer is important because it determines many properties such as stiffness, strength, viscoelasticity, toughness, and viscosity. Polymers with high molecular weight have higher resistance to the solvent dissolution, which has a direct influence on its viscosity [16].

For a polymer to be electrospun it must have sufficient polymer chains for it to undergo electrospinning, and it must have adequate solubility and preferably a rapid rate of dissolution. Dissolution is often a slow process. While some polymers dissolve easily in certain solvents, resulting in a real solution, other might need prolonged periods of heating at temperatures near the melting point of the polymer [11, 16] resulting in a quasi-solution.

2.2.4.3 Glass transition temperature (T_g)

Glass transition temperature is the temperature at which a polymer becomes brittle on cooling, or soft on heating. The glass transition temperature is a very important characteristic of polymers. This temperature defines the mobility state of the polymer molecules [16].

2.2.5 Electrospinning parameters

While the electrospinning setup and process itself may be relatively uncomplicated, the variables concerned in producing a nano-sized- diameter fiber mesh with relative uniformity are numerous. Process parameters include applied voltage, solution feed rate, and distance between the capillary and the collection screen. Ambient parameters include humidity, temperature, and airflow. System parameters include, the type of polymer, type of solvent, polymer concentration, solution viscosity, conductivity, and surface tension [16]. A diagram of electrospinning parameters is shown in Figure 2.6. Table 2.2 tabulates the various electrospinning parameters that should be considered in electrospinning.

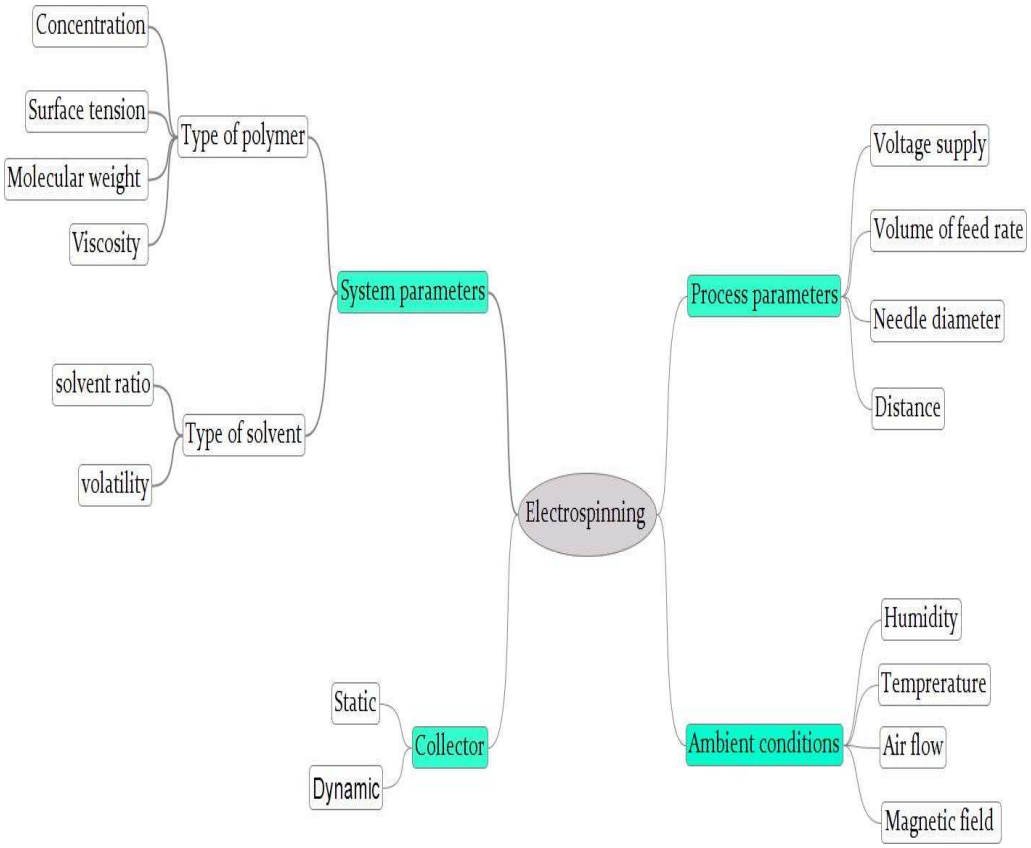

Figure 2.6: Diagram of electrospinning parameters [17].

Table 2-2: Summary of electrospinning parameters

Parameter	Description	Reference
Polymer concentration	Sufficient polymer chains need to be in the solution for it to undergo electrospinning. As polymer is added to a solution its viscosity increases and the solution may become too thick to be electrospun. Therefore, an appropriate polymer concentration and solution viscosity must be established. The fiber formation is largely dependent on the polymer concentration, which has a significant effect on the morphology, quality and diameter of the electrospun fibers.	[18, 19]
Viscosity	Viscosity is heavily influenced by polymer concentration. By increasing the polymer concentration, the number of polymer chains present in the solution will increase. The polymer solution is held in a droplet shape by surface tension. When the force from the electric field overcomes the surface tension, internal and external charges cause the liquid jet to be whipped around; this action causes the solvent in the solution jet to evaporate. System parameters must be optimized to create a solution that is able to be electrospun. Viscosity is an important practical parameter that must be controlled.	[18]
Conductivity	A spinning solution with high conductivity causes the diameter of the as-spun fibers to decrease. An increase in conductivity results in increased electrostatic forces on the jet and causes the jet to travel with greater velocity closer to the collector.	[14]
Surface tension	Surface tension is a property of the surface of a liquid that makes it act as an elastic sheet, and it reduces the surface area per unit mass of a fluid. The surface tension of a solution is directly influenced by the concentration of solvent molecules: at a high concentration of solvent molecules, the solution molecules take on a spherical shape as a result of the effect of the surface tension, which leads to the formation of beaded fibers.	[16,20,21]

Solution feed rate	Varying the solution feed rate is another way to control electrospun fiber diameters. When the flow rate is increased, there is a similar increase in the fiber diameter, simply because a larger volume of solution is drawn away from the spinneret per unit time.	[22]
Needle size	The diameter of the spinneret has a major effect on the size of the nanofibers produced. A smaller spinneret yields smaller fibers. The shape of the spinneret, i.e. whether the tip of the spinneret is flat or sharp also plays a major role in the electrospun sample.	[23-25]
Tip-collector distance	Several studies have shown that the further the spinning distance (between the anode and cathode), the finer the resulting fiber diameter will be. Increasing the distance will increases the amount of beading as a result of the effect of the electric field.	[26, 27]
Solvent	The type of solvent affects the electrospinning jet behaviour as well as the morphology of electrospun fibers. Solvents with low boiling points cause blockage of the capillary. The solvent should evaporate rapidly for the fiber to maintain its integrity when arriving at the collector plate, but not too fast, otherwise the fiber will solidify before it reaches the nano-scale.	[19]
Volatility and miscibility	It has been reported that highly volatile solvents often lead to the formation of pores on electrospun fibers.	[28]
Voltage supply	A high voltage is used to create an electrically charged jet of polymer solution. One electrode is placed in the spinning solution and the other is attached to a collector. Increasing the voltage reduces the amount of beading in the fibers.	[29]
Ambient humidity	If the relative humidity is less than 30 %, smooth fibers are produced and if the relative humidity is above 30 %, pores will begin to form on the surface of the fiber. An increase in the humidity will cause an increase in the number of pores on the surface. The presence of pores on the surface of electrospun fibers can serve to increase the surface area for filtration applications.	[30]

Dong et al. [31] have drawn attention to the effects of the solution properties on the morphology of the electrospun core-shell fibers. In their study they found that beaded fibers are often formed. They found that uniform fibers without beads were formed when using polystyrene (PS) with a molecular weight of 550000 g/mol. They demonstrated that the average diameter of the electrospun fibers was increased and that there was an overall reduction in bead formation when a higher polymer molecular weight and/or a high polymer concentration (120 mg/ml) in the spinning solution was used. The dielectric constant of the solvents was also studied and found that high dielectric constant of the solvent not only reduced the bead formation but also decreased the fiber diameter.

Son and Lee [29] reported on the effect of pH on the structural diameter of polyvinyl alcohol (PVA) fibers. They found that the conductivity of the PVA solution is strongly dependent on the pH, and as the pH is increased the average diameter of the PVA fiber significantly decreases. The viscosity and surface tension of a spinning solution however were not significantly affected by pH.

Yim and Shivkumar [32] found that the molecular weight of PVA has a significant effect on the system parameters, including electrical conductivity, viscosity and surface tension of the solution. They also found that the fiber diameter increases with increasing concentration of the polymer in the solution, and at each molecular weight that they studied there is a minimum concentration (9 wt %) needed to stabilize the fibrous structure and a maximum concentration (31 wt %) at which electrospinning becomes impossible.

A study by Gopal et al. [33] on electrospun nanofiber membranes (ENM), revealed that ENM are very attractive for separation technology, due to their high flux, high surface area and high separation efficiency (small pores and interstice size and structure). They demonstrated that the overlapping nanofibers, when collected as random fiber arrays, offered more open pore structures, which are ideal for separation membranes. They also demonstrated that, in membrane applications, the electrospun fibers require additional support to provide strength and stability to the membrane. In the case of micro-particle separation they found that for 5 µm particles the separation efficiency was 91%, which was lower than for 10 µm

particles, where the separation efficiency was 96%. When a membrane has pores larger than 5 µm some of the particles will permeate through the ENM.

It can be concluded from the literature that the ability of the spinning solution to be successfully electrospun is dependent on its concentration, electrical conductivity, viscosity and surface tension, and also general parameters such as spinning distance, voltage applied, and type of solvent used.

2.6 Mathematical model identifying the behaviour of an electrospinning jet

Various models have been developed for the creation of jets and their behaviour. They successfully illustrate the nonlinear behaviour of the whipping mode in the unstable region of the jet [34, 35]. Fridrikh et al. [34] proposed a model describing the effect of the jet diameter on the final fiber diameter that is formed during the electrospinning process as a function of the system and process parameters (the conductivity, dielectric permeability and dynamic viscosity of solution, the surface charge density and surface tension) [36]. See equation 2.1. The model includes a comprehensive list of parameters that an experimental setup could or should consider. This model is confined by two assumptions. The first assumption is that the liquid is Newtonian, and neglects the elastic effect due to the evaporation of the solvent. Thus this model showed a good agreement with experimental results obtained for polyethylene oxide (PEO) and polyacrylonitrile (PAN) solutions with high boiling solvents, but not with polymer solutions with volatile solvents. The second assumption is that no further thinning occurs after the terminal jet formed. Nevertheless, this model was accepted by the electrospinning community as it gives an uncomplicated analytical methodology [37].

$$h_t = \left[\gamma\varepsilon \frac{Q^2}{I^2} \frac{2}{\pi(2\ln x - 3)} \right]^{\frac{1}{3}} \qquad 2.1$$

where h_t is the final jet diameter (m), γ is the surface tension (dyne/cm), Q is the flow rate (m^3/s), I is the electric current (Coulomb/s) , ε is the dielectric permittivity, and x is the displacement of the centreline of the jet.

Figure 2.7 shows the nonlinear behaviour of the whipping mode in the unstable region.

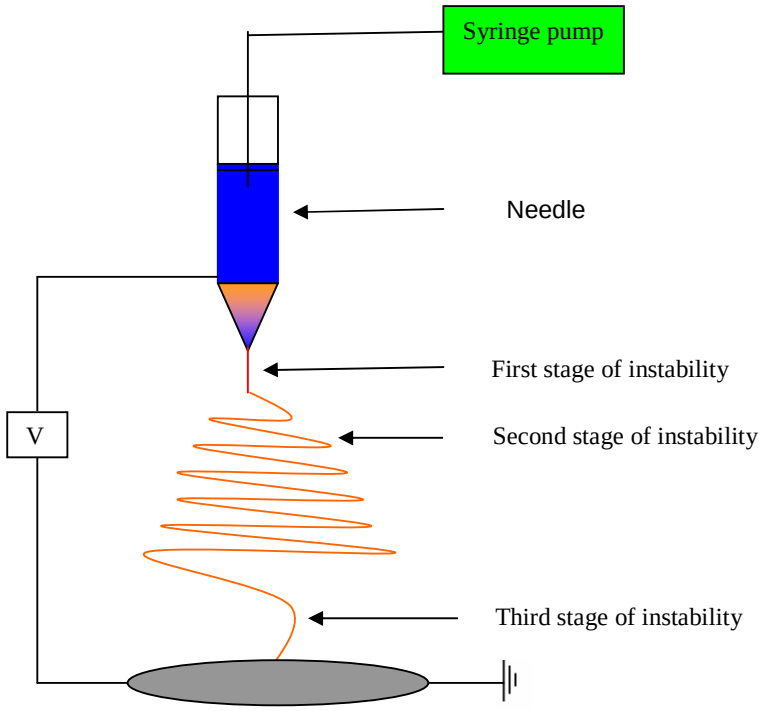

Figure 2.7: Typical trajectory of a moving jet in electrospinning process.

The one- dimensional steady model for an electrospinning jet pulled from a capillary orifice and modified by a constant external electric field is described [38].

The model describes the steady state flow of an infinite viscous jet pulled from a capillary orifice and accelerated by a constant external electric field.

The current balance in the jet can be expressed by the following equation:

$2 \pi r \sigma u + \pi r^2 kE = I$ [38] 2.2

The conservation of mass equation is expressed as: $\pi r^2 u \rho = Q$ [38] 2.3

The force balance is expressed as: $d/dz\ (u^2/2) = (2\sigma E/\rho r) + 1/\rho\ (d\tau/dz)$ [38] 2.4

(the last term of right side of Eq. (2.4) is the viscous force)

The length of the straight jet in electrospinning process is expressed as

$$L = \frac{4kQ^3}{\pi \rho^2 I^2}\left(R_0^{-2} - r_0^{-2}\right) \qquad 2.5$$

where r is the radius of the jet (m), σ is the surface density of the charge (Coulomb/m^2), u is the velocity (m/s), k is the electrical conductivity of the fluid, I is the current (Coulomb/s), Q is the mass flow rate (kg/s), ρ is the liquid density, E is

the applied voltage, τ is the viscous force, L is the length of the straight jet and R is the principle radius curvature. The equations (2.2, 2.3, 2.4 and 2.5) are limited to the initial stage of the electrospinning which provide rational theory that can simply predict the length of the straight jet (Figure 2.7) in electrospinning.

Many analytical relationships between the radius of a jet (r) and the axial distance from the nozzle (z) have been investigated since the electrospinning process was first patented by Formhals in 1934. Spivak et al. [35, 39] created the following model for a steady state jet in the electrospinning process.

$$\frac{d}{dz}\left[R^{-4} + (WeR)^{-1} - Eu^{-1}R^{2} - Re^{-1}(dR^{-2}/dz)^{m}\right] = 1 \qquad 2.5$$

$$R \sim z^{-1/4} \qquad 2.6$$

The Weber number describes the ratio of the surface tension forces to the inertia forces.

$$We = \left(2\pi^{2}R_{o}^{3}\gamma\right)/\left(\rho Q^{2}\right) \qquad 2.7$$

The Euler number describes the ratio of the electric forces to the inertia forces.

$$Eu = \left(\pi^{2}I^{2}R_{o}^{6}\right)/\left(4\varepsilon_{o}\,\rho Q^{4}\right) \qquad 2.8$$

The Reynolds number describes the ratio of the inertia forces to the viscous forces.

$$Re = \left(\rho Q^{2}\right)/\left(2\pi^{2}R_{o}^{4}\,\eta\right)\left[\left(4\pi E_{o}IR_{o}^{2}\right)/\left(\rho Q^{2}\right)\right]^{-m} \qquad 2.9$$

Where R is the dimensionless jet radius ($R^{\sim} = R/R_o$) and the R_o is usually taken equal to the radius of the capillary orifice, z is the dimensionless axial coordinate ($z^{\sim} = z/z_o$), We, Eu and Re are, respectively the Weber, Euler, and Reynolds numbers. σ is the surface density of the charge (Coulomb/m^2), I is the current (Coulomb/s), Q is the mass flow rate (kg/s), ρ is the liquid density, γ is the surface tension forces, E is the applied voltage, ε is the dielectric permittivity and m is the flow index (Pseudoplastic shear thinning fluids are described by the flow indices ($0 \leq m < 1$).

Baumgarten [40] highlighted the effect of solution viscosity on the fiber diameter and jet length. In his study he found that increasing the solution viscosity resulted in an increase in fiber diameter. Baumgarten obtained the following equation: $D = \eta^{0.5}$ where D is the fiber diameter (nm) and η is the solution dynamic viscosity (in poise).

All the above discussed mathematical models are still under development and haven't been widely used in electrospinning. These mathematical models are based

on general mathematical, fluid dynamic and physical principles, which can be used for better control and optimization of the electrospinning process.

2.7 Co-electrospinning

By modifying the spinneret design, different properties can be introduced to the fiber. Coaxial spinneret designs have been employed by various researches for various aims in electrospinning. There has been much research recently on coaxial electrospinning [41] and control of the fibers at the submicron and nanometre scale where various polymers have been successfully electrospun into nano-scale core-shell fibers by using a coaxial spinneret. Table 2.3 shows selected polymers that have been electrospun into core-shell fibers. The co-electrospinning setup (Figures 2.8) comprises a compound spinneret, consisting of two small-diameter capillary tubes with one located inside another. In the coaxial spinneret design the liquid is driven to the needle tip by a syringe pump forming a droplet at the tip. A high voltage supply is used to create an electrostatic charged jet of the polymer solution, where one electrode is placed in the spinning solution and the other attached to a collector.

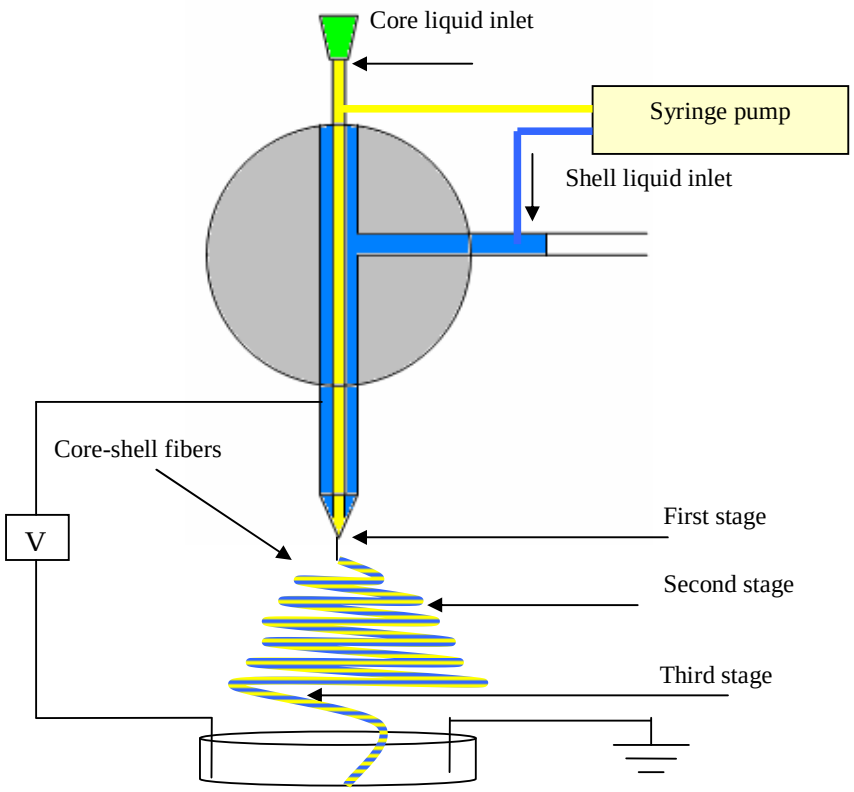

Figure 2.8: Schematic of the co-electrospinning setup.

Table 2-3: Selected polymers that have been electrospun into core-shell fibers

	Polymer	Solvent	Polymer content (wt %)	Flow rate (ml/hr)	Electric voltage (kv)	Collector distance (cm)	Needle diameter (mm)	Fiber diameter (μm/nm)	Ref.
Shell	PAN	DMF	12	0.2	0.3 KV/cm	18	1.2	7.3 μm	[42]
Core	PMMA	Acetone/ DMF	15	0.6	–	–	0.42	2.1 μm	
Shell	PCL	Chloroform /DMF	10	4	0.5 KV/cm	16 ~20	0.8~0.9	several micrometer	[43]
Core	PEO	Ethanol/ water	4	0.5	–	–	0.4~0.5	–	
Shell	PCL	–	–	1.8	10.1	13 cm	2.5	380 nm	[28]
Core	Fitc BCA/ PEG	Deion. water	–	0.2	–	–	1.1	270 nm	
Shell	PCL	–	120 mg/ml	2	11	14	2.5	100-500 nm	[44]
Core	Fept	Hexane	5 mg/ml	0.4-0.8	–	–	1.1	20-50 nm	
Shell	SOG/PVP	–	15	10 μl /min	4.3	7.3	1.07	59~60 nm	[45]
Core	Motor oil	–	–	2 μl /min	–	–	0.11 mm	–	
Shell	PC	THF/DMF 1:1	20	2	21	12-13	–	177-1813 nm	[46]
Core	PU	THF/DMF 1:1	4,6,8,10	1.5	–	–	–	–	
Shell	Gelatin	glacial aa	9-12% wt/vol	300-500 μl /hr	–	–	–	–	[47]
Core	PCL	glacial aa	–	300-500 μl /hr	–	–	–	–	
Shell	PEO	water	5	_	_	_	_	160 nm	[48]
Core	PASA	_	_	_	_	_	_	30 nm	

Shell	Somos	_	_	12	7.5	2.5	1.1	_	[22]
Core	Ethylene-glycol	_	_	0.3	_	_	0.5	_	
Shell	PCL	DMF/ chloroform	300 mg/ml		15.2	40	0.9	774-545 nm	[23]
Core	PEG	_	10	0.6-2	_	_	0.57	80-311 nm	
Shell	PVP/ $Ti(OiPr)_4$	Ethanol	0.03/0.5 g/ml	0.6	12-16	9	450 um	200-130 nm	[49]
Core	Mineral oil	_	_	0.03-0.3	_	_	100 um	_	
Shell	PVP/TiO_2	Ethanol / aa	6%:25% w/v	0.01	15	10	_	85-350 nm	[50]
Core	Mineral oil	_	_	0.005	_	_	_	–	
Shell	PCL	Dichloromethane/ ehtanol	10	3	10-15	5	_	484 nm	[51]
Core	BSA	_	_	1	_	_	_	250 nm	

Polymers

BCA: Base surfactant
Fept: Iron-platinum
Fitc: Fluorescent isothiocyanate
PAN: Polyacrylonitrile
PASA: Poly (aniline sulfonic acid)
PC: Polycarbonate
PCL: Poly(caprolactone)
PEG: Poly(ethylene glycol)
PEO: Poly(ethylene oxide)
PMM: Poly(methyl methacrylate)
PU: Polyurethane
PVP: Poly(vinyl pyrrolidone)
SOG: Silicon-on-glass
Ti(OiPr): Tetraisopropyl orthotitanate
TiO_2: Titanium dioxide

Solvents

DMF: dimethlyformamide
THF: tetrahydrofuran
aa: acetic acid
Deion.water: deionized water

–: data not available

Table 2-3 tabulated more than twenty two different polymers that have been successfully electrospun into core-shell fibers with diameter ranging from 60 nm to over 7 μm, and from 20 to 2 μm shell and core respectively. Most of the polymers

were dissolved in the solvents (see Table 2.3) before electrospinning. The polymer is completely dissolved in an amount of solvent in a glass container (called polymer solution). It is noted that the same polymer dissolved in different solvents may all be electrospun into nanofibers. For a polymer to be electrospun it must have sufficient polymer chains for it to undergo electrospinning, and it must have adequate solubility and preferably a rapid rate of dissolution. A DC voltage in range of 5 to 25 kV is necessary to generate the electrospinning.

2.7.1 Production of core-shell polymer nanofibers by co-electrospinning

There has been much research recently on co-electrospinning and control of the fibers at the submicron and nanometre scale where various polymers have been successfully electrospun into coaxial fibers upon the generation of electrified coaxial jets instead of single jets.

McCann et al. [12] reported that they were able to produce ceramic hollow nanofibers by using two coaxial capillaries. The design of the set-up for their experiment was similar to the conventional electrospinning design, except for the use of a spinneret containing two coaxial capillaries. The spinneret was manufactured by inserting a polymer-coated silica capillary with an inner diameter of 100 µm and an outer diameter of 200 µm respectively. They demonstrated that hollow nanofibers with a core and a shell could be conveniently fabricated by electrospinning two immiscible liquids through a coaxial two-capillary spinneret. They also demonstrated that the hollow nanofibers could be obtained as uniaxially aligned arrays with lengths up to several centimetres, by modifying the collector (that involved the use of a rotating drum or a pair of split electrodes as the collector). Additionally they found that the hollow nanofibers could be well separated from each other and be conveniently transferred onto other substrates for a variety of applications [12].

Dong et al. [31] successfully produced electroactive PAN/PMMA coaxial fibers. They found that solution properties, including the polymer molecular weight, solution concentration, solvents, dielectric constant, and the solution ionic strength strongly affected the morphology and the diameter of the electrospun fibers. They also found that a high polymer molecular weight and a high solution concentration

resulted in the formation of large fibers without beads. Furthermore, they demonstrated that the addition of an organic salt led to less bead formation (by increasing the charge density in the pendant droplet) and the solvent dielectric constant substantially influenced both the morphology and the diameter of the fibers.

Li et al. [52] fabricated core-shell and hollow nanofibers but they could not obtain a stable jet due to the break-up of the jet. They solved this problem by using two co-spinning immiscible solutions. During their research they found that using a sol-gel precursor and gelatine during the spinning process prevents fiber break down, resulting in stable fiber morphology. They also found that using a coaxial spinneret to make multi-shell nanofibers using two capillaries was practical [52].

A study by Lallave et al. [53] on the production of hollow carbon nanofibers by coaxial electrospinning of Alcell lignin polymer (without binder) demonstrated that an applied high voltage between the spinneret and collector, with one electrode placed in the spinning solution and the other oppositely attached to a conductive collector, provided better electrostatic conditions to prevent fibers from flying to any grounded piece near the set-up. To generate hollow nanofibers, they used a tri-coaxial electrospinning method. The purpose of the outer capillary needle was to allow a thin sheath of ethanol to flow to compensate for solvent losses caused by the evaporation of the lignin solution in the Taylor cone. They also demonstrated that by controlling the shell solutions flow rate ratio, one can switch from steady electrospinning to steady electrospraying.

Bazilevsky et al. [54] introduced a single nozzle co-electrospinning technique using blends of PMMA/PAN solutions in DMF. The as-spun fibers featured a core-shell structure similar to that produced by coaxial nozzles. The following conditions are required to achieve co-electrospinning by this approach: 1) rapid, solidification of the shell solution; 2) good wetting of the shell by the core solution (it is preferable to use a core solution containing a known solvent to the shell polymer); 3) it is recommended that a viscoelastic polymeric core solution be used in order to achieve a stabilized co-electrospinning process; 4) the shell to core solution feed rate ratio should be chosen according to the required diameter of resulting fibers. [Carbonization of such fibers yielded multiwalled carbon nanotubes].

Wang et al. [45] produced oriented and circular silica nanochannels (nanotubes) and demonstrated their application for single molecule detection. Their approach needed a specially designed coaxial spinneret, with two independent syringes placed in an L shape having an inside diameter of 1.07 mm for the shell needle and 0.11 mm for the core needle (Table 2-3). In their study SOG/PVP was used as shell fluid and motor oil as the core fluid, they found that the effect of the core feed rate on the ID of the electrospun nanochannels was significant. They demonstrated that when the feed rate of the motor oil varied from 2 to 6 μl/min, with a feed rate of 10 μm/min for 5 wt % PVP in SOG and the electric field of 525 V/cm kept constant, the average ID of the electrospun nanochannels increased from 29.8 to 39.25 nm. Additionally, they found that at a low feed rate of motor oil no continuous core shell fibers were formed. This was due to the low pressure of motor oil that was insufficient to balance the viscous stress of the wall material. On the other hand, if the core feed rate was too high the nanochannels would collapse due to the break-up of the interfacial layer between the core flow and shell flow.

2.8 Hollow fiber membranes

The exceptional mass transfer efficiency and good performance of hollow fiber configurations provided it with a range of applications in various fields including food, juice clarification, dairy processing, medical fields, gas separation biochemical industry and most recently municipal drinking water [55]. The advantages of the hollow fiber that make it attractive in these applications are summarized below [56]:

- large surface area per volume ratio
- lower chemical costs
- reduced waste disposal
- deliver of higher quality product water
- decreases labour costs
- reduce space requirements
- flexibility in system design and operation
- structural integrity and construction

Fabrication of hollow fibers using the coaxial electrospinning technique was first established by Li and Xia [49] . Heavy mineral oil and olive oil (non-polymeric

liquids) were used as the core material. Li and Xia used polyvinylpyrrolidone (PVP) and a ceramic precursor $Ti(OiPr)_4$, in ethanol as the shell solution and mineral oil as the core. The oil was extracted using octane. According to the authors, the inner diameter and the wall thickness of the electrospun hollow nanofibers can be varied by varying the feed rate of the core fluid. They also demonstrated that using two immiscible solutions is essential to produce successful hollow fibers and also to guarantee that both core and sheath solutions do not mix in the course of the spinning process.

In the review article, Moghe and Gupta [57] reported that the shell material could act as a template and leader for the core material to form woven fibers, even if the core material was not electrospinnable. They also reported that some materials are non-electrospinnable due to their low molecular weight, limited solubility, unsuitable molecular arrangement or lack of required vicoelastic properties.

2.9 Applications of electrospun nanofibers

The Nanofibers have potential applications in filtration of submicron particles in the separation industries, catalysis, biomedical applications, pheromone-release systems for crop protection, wound dressing in the medical industry and tissue engineering (tissue engineering is the field that applies the principles of biology and engineering to develop tissue substitutes to restore, maintain, or improve the function of infected or damaged human tissues) (Figure 2.9) [58]. To date nanofiber membranes, tissue engineering, medical industry and textile industry provide the most important applications for nanofibers. Figure 2.10 shows the total number of publications and patents for electrospinning nanofibers for each year from 1996 through 2008. The largest annual increases in electrospinning nanofibers research were between 2005 and 2008.

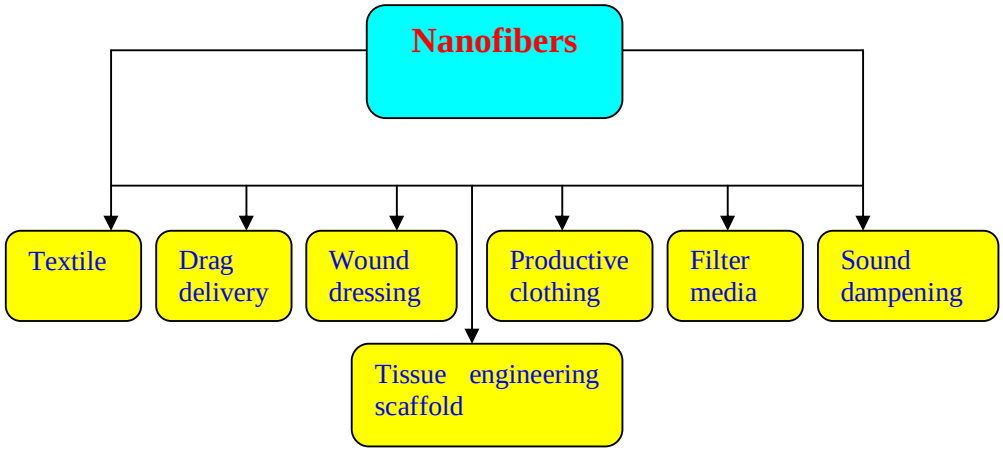

Figure 2.9: Application fields based on publications and patents on electrospun nanofibers.

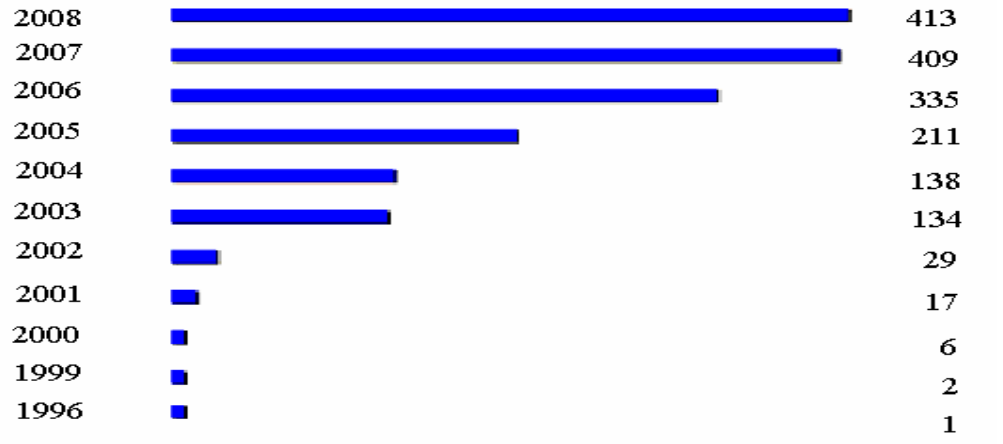

Figure 2.10: The total number of publications and patents for electrospinning nanofibers for each year from 1996 through 2008.

2.9.1 Filtration

Recent research has resulted in the development of a high-tech nanoscale fiber spinning process for the production of high performance nanofibers capable of being used for the filtration of contaminants and biological agents [13].The filtration process can be divided into two stages: In the first stage (referred to as the stable stage) the efficiency, performance and resistance remain constant during the filtration process. In the second stage (the unstable stage) the resistance and the efficiency of the filtration process are strongly influenced by deposited particles. The first stage is the principal one. Nanofibers filters link up with the first stage [1].

2.9.2 Cellulose acetate membranes

Cellulose acetate was first prepared in 1865 by Paul Schutzenberger [59]. Cellulose has been widely used for fibers and films. Good thermal stability, biodegradability and chemical resistance are the most important properties of cellulose acetate nanofiber membranes. These properties opened a wide range of applications for cellulose acetate affinity membranes (selective membranes): film base in photography, biomedical films, and components in some adhesives and as semi-permeable membranes for water filtration [60].

The separation process for membranes is based on two factors, selectivity and flux. Selectivity is determined by the surface and bulk properties of membrane material that define the character of species that can be pass through, whereas flux identifies the rate at which the species are transported across or through the membrane. The two determining factors are strongly influenced by the morphology and structure of the membrane, which includes the porosity, wettability, thickness and pressure drop across the membrane [3].

2.10 Summary

Electrospinning is a novel processing technique for the production of fibers with diameters in the range of a few nanometres to tens of micrometers. These fibers are smaller than those produced by conventional spinning, including wet spinning, dry spinning and melt spinning. Electrospun nanofibers membranes have several attractive attributes that make them very attractive in many applications, particularly those requiring high porosity (pore size), high permeability, and large surface area per unit volume.

Co-electrospinning has gained much attention in recent years and is potentially useful in a variety of applications. In the co-electrospinning design the two fluids are pumped, independently, to the coaxial spinneret by syringe pumps, forming nanofibers in a core-shell configuration. According to literature there are a few parameters that affect the diameter of electrospun fibers more than others: polymer concentration, type of solvent, solution feed rate and spinning distance. These parameters are in general, in the range of 5 to 25 wt % polymer concentration, 1:1 to 1:5 solvent ratio, 0.1 to 7 ml/hr solution feed rate and from 8 to 25 cm spinning distance.

Chapter 3

Materials and Methods

3.1 Materials and equipment

3.1.1 Materials

Cellulose acetate (CA) was selected as the model membrane material as it is commonly used in microfiltration and ultrafiltration membranes and because of the overall advantages of its properties, such as the cost, highly hydrophilic, and the ease of use.

The following materials were used in this study: cellulose acetate (shell material), with an acetyl content of 39.9 %, (Eastman Kodak, Rochester N.Y.); mineral oil (core material) density 0.88 g/ml (Saarchem, SA); octane (Merck-Schuchardt), acetone (Sasol, SA); and dioxane from (British Drug House, England). All were used as received without any further purification. Table 3.1 tabulates some of the properties of the chemicals used in this study.

Table 3-1: Properties of solvents used in this study

Solvent	Density (g/ml)	Boiling point (^{o}C)	Vapour pressure (atm) at 20 ^{o}C
Acetone	0.78	56.2	0.242
Dioxane	1.033	101.1	0.038
Octane	0.70	126	0.014

3.1.2 Equipment

The following equipment was used in the electrospinning setup: a coaxial needle obtained from VICI AG International (Switzerland), pump 33 dual syringe pump obtained form Harvard Apparatus (USA) and a 30 kV high power voltage supplier obtained from the Electrical Engineering Department (Stellenbosch University). Both the electrospinning setup and the coaxial needle (Figures 3.1 and 3.2) were designed as part of this study. The coaxial spinneret designed consists of two small concentric needles, one located inside another, having internal diameters of 0.3 and 1.2 mm for the inside and outside needles, respectively.

Equipment that was used in the electrospinning setup is tabulated in Table 3.2.

Table 3-2: Equipment used in the electrospinning setup

Items	**Source**
Syringe pump model 33	Harvard Apparatus (USA)
Coaxial needle	VICI AG International (Switzerland)
High power voltage suppler	Electrical Engineering Department, Stellenbosch University (SA)

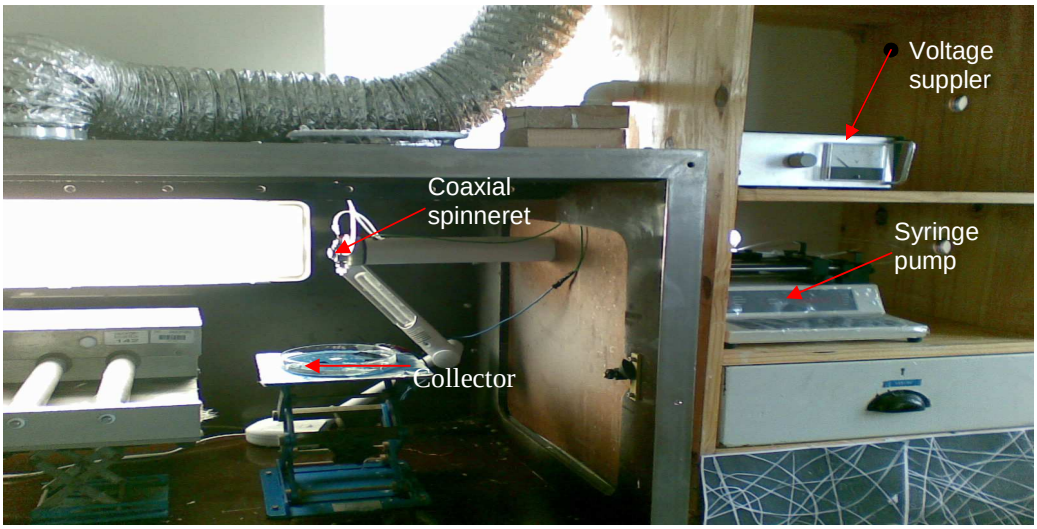

Figure 3.1: Photograph of electrospinning equipment used in this study.

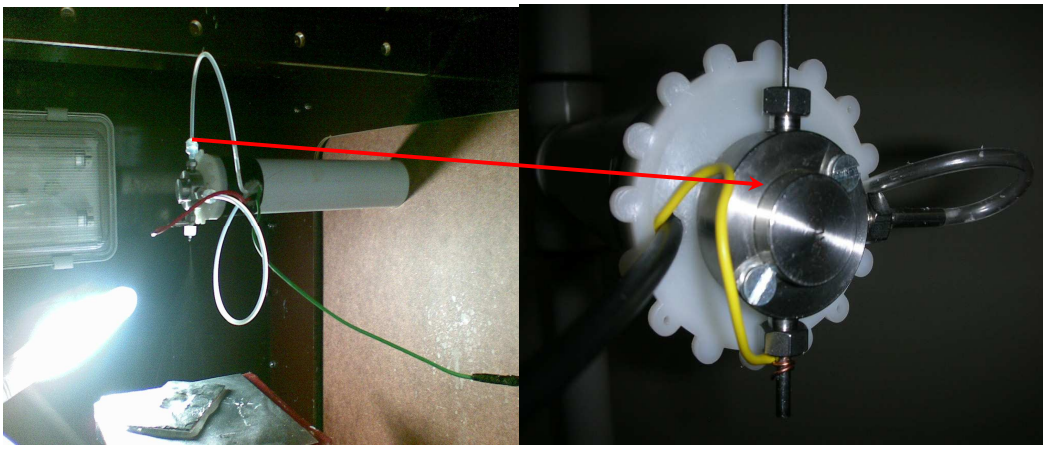

Figure 3.2: Photograph of coaxial spinneret used in this study.

3.2 Selection of solvent for CA solution spinning

In order to prepare solutions suitable for electrospinning CA fibers, various solvents and solvent systems were studied, including: acetone, dimethylacetamide, dioxane, methanol, acetic acid, ethanol, water and ethylene chloride. All the spinning solutions were stirred on a magnetic stirrer plate for 24 hours at room temperature until the solutions became homogeneous, and then the container with the solution was sealed and stored at room temperature until use. Some changes in the viscosity of the solutions were visible after a period of 72 hr.
Solvent systems that were studied are listed in Table 3-3.

Table 3-3: Solvent used for cellulose acetate and solution concentration considered in this study

Solvent	**Solvent ratio**	**CA (wt %)**
Acetone/DMAc	1:1, 2:1, 3:1	10; 12; 15; 17
Acetone/methanol	1:1, 2:1	12
Acetone/ethanol	2:1	12
Acetone/methanol/ethanol	2:1:1	12
Ethylene chloride/ethanol	80:20	10
Acetic acid/ water	80:20	16
Dioxane/acetone/methanol/ maleic acid	45.1: 28.7: 7.2: 2.4	16.4
Acetone/ Dioxane	2:1	12; 15

3.3 Determination of solution properties

3.3.1 Solution viscosity

Dynamic viscosity is the property of the liquid that presents the resistance of the liquid to flow. In electrospinning, dynamic viscosity is the factor that determines the “spinnability” of the solution. The viscosity of a polymer solution having a high molecular weight will be higher than that of a polymer solution with low molecular

weight. One of the conditions essential for electrospinning to occur where fibers are produced is that the polymer solution must consist of a polymer of sufficient molecular weight (the chain entanglements should form continuous fibers when an electric field is introduced to the polymer solution) [19]. When the correct viscosity of the spinning solution is achieved the Taylor cone will form, resulting is a stable coaxial jet.

A Physica MCR 501 (Figure 3.3) rheometer was used to determine the dynamic viscosity of an electrospinning solution. The changes in dynamic viscosity and shear stress with change in shear rate were measured. A computer recorded the resulting shear rate vs. viscosity data. Figure 3.4 shows the viscosity measurements vs. shear rate data for the four CA solutions that were successfully electrospun. The relationship between shear rate and the viscosity was investigated and this information was then used to report on the dynamic viscosity of the solutions.

Figure 3.3: Picture of Paar Physica MCR 501 modular compact rheometer used to measure the viscosity of polymer solutions.

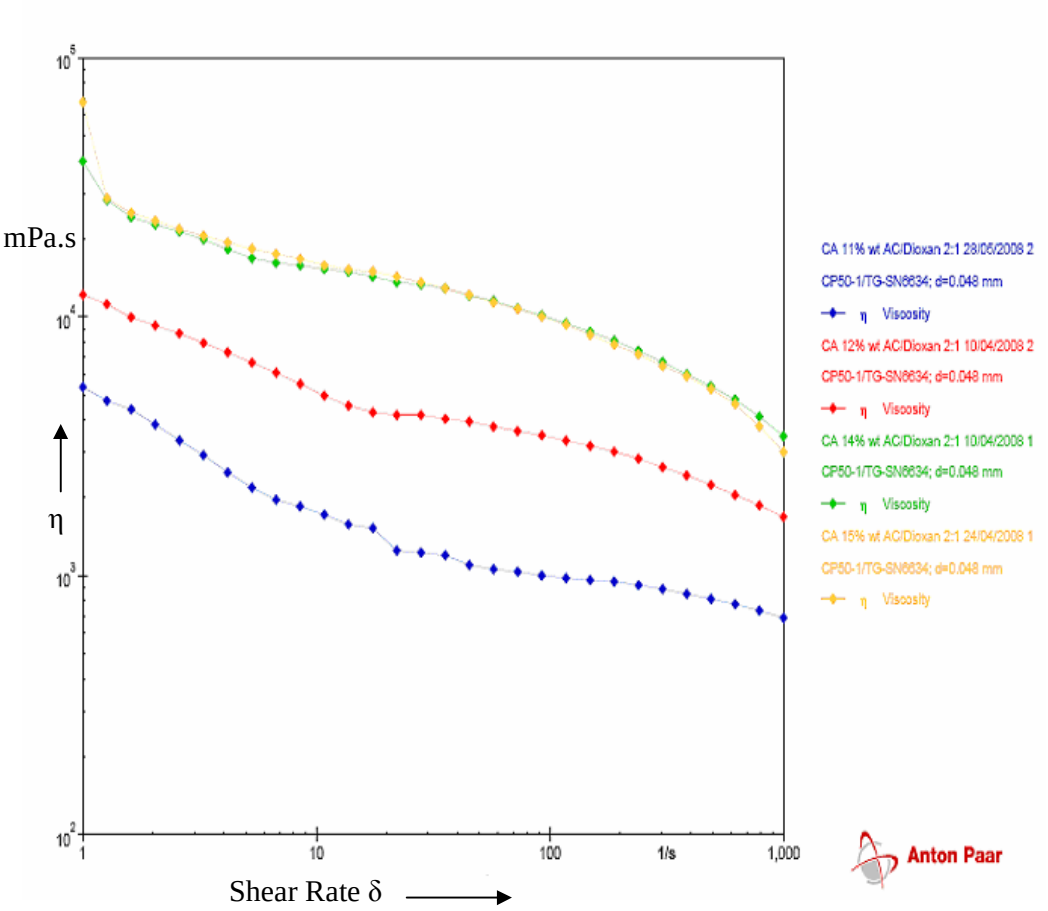

Figure 3.4: Flow curve for CA solutions at different concentrations; viscosity vs. shear rate.

Fluids such as water, air, ethanol and benzene are Newtonian. Solutions of low molecular weight substances are usually also Newtonian, such as a aqueous solution of sugar or salt [61]. Any fluid that does not obey the Newtonian relationship between the shear stress and shear rate is called non-Newtonian. When the viscosity decreases with increasing the shear rate, the fluid is called shear thinning. In the opposite case, where the viscosity increases with increasing shear rate the fluid is called the shear-thickening [61]. The plot of shear stress versus shear rate of 14 wt % CA in Figure 3.5 is similar to that of a plot of pseudoplastic fluids in Figure 3.6.

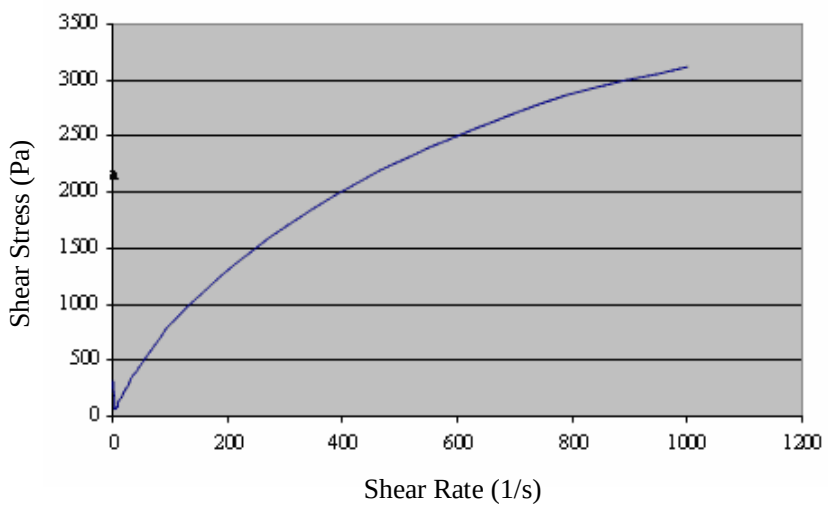

Figure 3.5: Plot of shear stress with shear rate of 14 wt % CA solution.

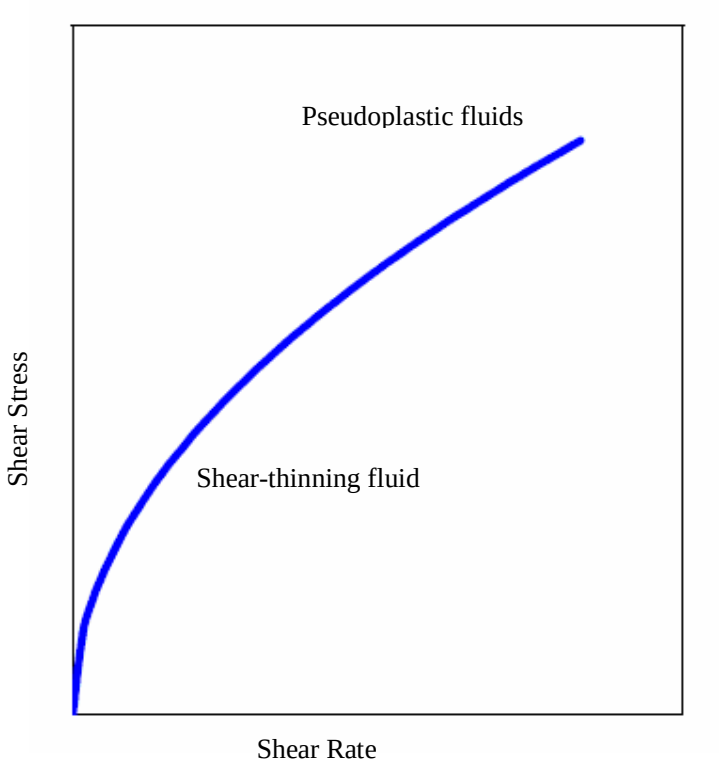

Figure 3.6: A typical shear stress versus shear rate plot for a shear-thinning fluid [61].

.

When the viscosity is plotted against the log shear rate, the following curve is obtained.

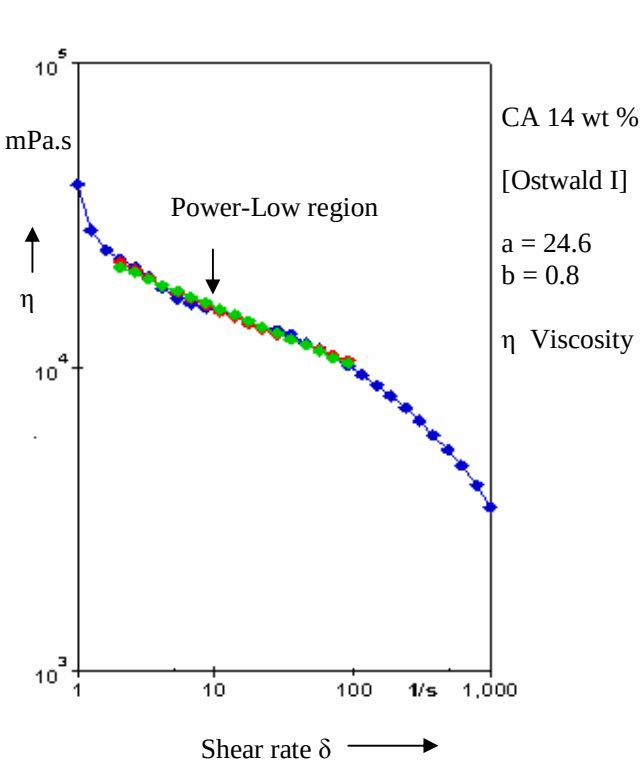

Figure 3.7: Flow curve of 14 wt % CA solution: viscosity vs. shear rate.

The two regions where the viscosity is approximately constant are known as Newtonian regions. The region between these two regions is usually approximated by a straight line on these axes and is known as the power-law region [61]. In this region, the behaviour can be approximated by

$$\ln \eta = \ln a + b.\ln \delta \qquad 3.1$$

$$\eta = K \delta^{b} \qquad 3.2$$

where η is the shear viscosity of the fluid, δ is the shear rate, K (intercept) = exp (a), and b can be expressed as (n-1) where n is called the power-low index. For a shear thinning fluid $n < 1$ [61].

The experimental data obtained have been fitted with the Ostwald's model [62].
An Excel spreadsheet showing all calculations and results of the viscosity measurements of the CA solutions of the four different concentrations is given in Appendix B (Table B1).

As the spinning solutions concentrations of 11, 12, 14 and 15 wt % CA in acetone:dioxane 2:1 solvent ratio were found the most suitable concentrations, because it allowed continuous electrospinning, they were the solutions that were used for viscosity measurements. At a given shear rate the viscosity of all these solutions was found to decrease with an increase in the shear rate. This indicated the fluid is shear-thinning fluid (pseudoplastic fluid). Table 3-4 tabulates the shear viscosity of the four selected CA solutions at different shear rates.

Table 3-4: Shear rate and shear viscosity of CA solutions in acetone: dioxane (2:1)

CA concentration (wt %)	Shear rate (1/s)	Shear viscosity (Pa.s)
11	17.4	1.55
	22.1	1.41
	28.1	1.31
	35.6	1.21
12	17.4	4.85
	22.1	4.56
	28.1	4.28
	35.6	4.02
14	17.4	14.2
	22.1	13.6
	28.1	13.0
	35.6	12.4
15	17.4	14.6
	22.1	13.9
	28.1	13.2
	35.6	12.6

The results of the viscosity measurements of the CA solutions of the four different concentrations showed that the samples with initial viscosity values ($\eta < 4$ Pa.s at shear rate of $\delta > 35$ 1/s) the solution drip rate from the spinneret was markedly higher, while the samples with viscosity values ($\eta > 14$ Pa.s at shear rate of $\delta < 17$ 1/s) did not spin. It would thus appear that CA solutions with a viscosity of between 4 and 15 Pa.s are required for electrospinning.

3.4 Determination of the molecular weight of CA via Gel Permeation Chromatography (GPC) analysis.

GPC is essentially a process for the fractionation of polymers according to their size and gives the molecular weight distribution. GPC analysis is performed using a column that is packed with polystyrene and the molecules are separated according to their molecular size and shape. [CA was dissolved in THF and introduced into the GPC column using a syringe]. The molecular weights of a sample are calculated from a standard curve based on model compounds. The weight-average molecular weight (M_w), number-average molecular weight (M_n), z-average molecular weight (the distribution of the large molecular) (M_z) and polydispersity index (PDI) of CA were determined (with respect to polystyrene calibration standards). Results are tabulated in Table 3-5. The GPC curve (Figure 3.8) of the CA shows a dominant peak at a retention time of 13 min with molecular weight around 126999.

Table 3-5 shows that $M_z > M_w > M_n$ and polydispersity >1. The polydispersity is high, indicating that CA has a wide molecular weight composition range.

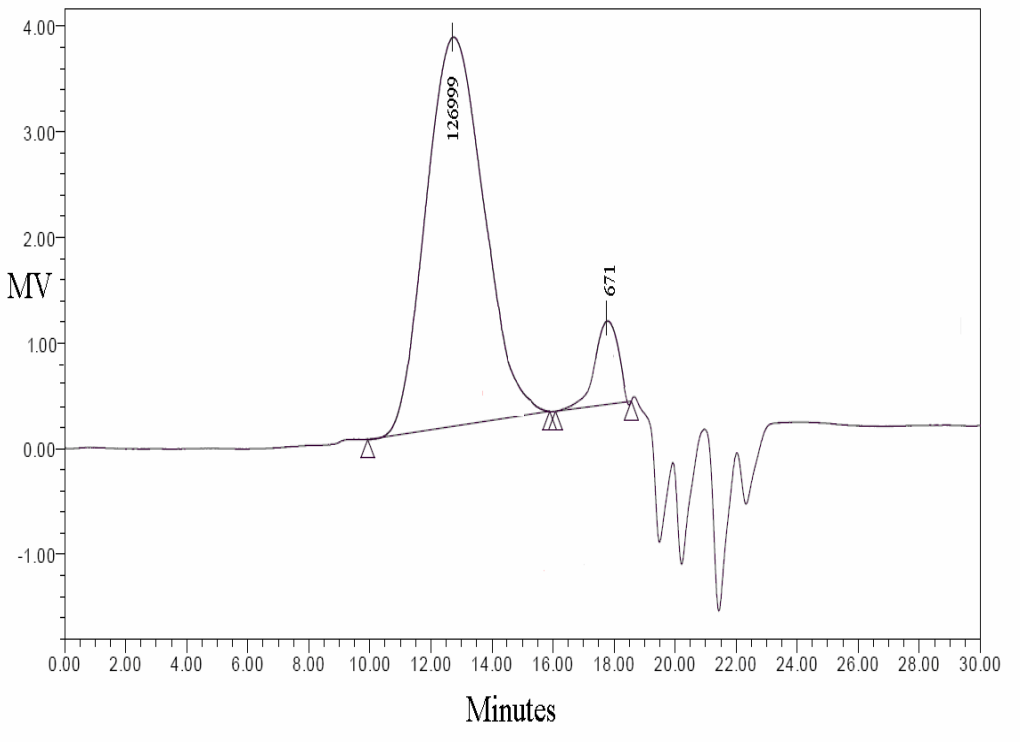

Figure 3.8: The molecular weight distribution curve of the CA measured by GPC.

Table 3-5: Statistical distribution of molecular weight of the CA measured by GPC

Mn (Daltons)	Mw (Daltons)	Mp (Daltons)	Mz (Daltons)	Mz+1 (Daltons)	Polydispersity	Mz / Mw	Mz+1/ Mw
69927	162731	126999	318638	511549	2.32	1.95	3.14
		671					

3.5 Experimental procedure for co-electrospinning of CA to form hollow fibers

3.5.1 Operating parameters

As mentioned earlier (section 2.2.4) there are many parameters that influence the structure and properties of the electrospun polymers. All these parameters have been widely reported in the literature (see Table 2.2 in section 2.2.4). Consideration was given to various operating parameters for the electrospinning process: solution concentrations, solvent ratios, voltages, spinning distances, and feed rates were studied and evaluated in efforts to achieve stability of the electrospinning process and produce uniform fibers. Table 3-6 tabulates the ranges of operation parameters (based on an extensive literature review) used in the co-electrospinning of CA hollow fibers.

Table 3-6: Ranges of the operation parameters used for co-electrospinning

Parameters	Operation values	Reference
Collector distance	5-20 cm	[26,27,43]
Core feed rate	0.01-5 ml/hr	[28,44,50,57]
Shell feed rate	1-10 ml/hr	[28,44,50,57]
Solution concentration	11-16 g/ml	[60,59]
Solent ratio (acetone:dioxane)	1:1; 2:1,3:1; 5:1 v/v	[59]
Humidity and temperature	45-55/25 ^{o}C	[30]
Voltage	10-25 kV	[29,41]
Core needle inside diameter	0.3-1 mm	[28,41]
Shell needle inside diameter	1.2-2 mm	[28,41]

3.5.2 Co-electrospinning of CA to form hollow fibers

The co-electrospinning setup used (Figure 3.10) comprised of a compound spinneret, consisting of two concentric small-diameter capillary tubes/needles, one located inside another (core-shell/co-axial design), and having internal diameters of 0.3 and 1.2 mm for the inside and outside needles, respectively and 0.3 mm shell/core gap (see Appendix E, Figure E1 for the specific mechanical design). A 10 ml syringe was used to pump the solution directly to the spinneret. The liquids (CA-shell/mineral oil-core) are pumped to the core-shell needle tip by a dual syringe pump. Plastic tubing (polypropylene, inner diameter 1.5 mm, approximately 15 cm in length) was used to connect the syringes to the capillary. A high voltage source was used to apply a potential of several kilovolts over the electrospinning distance. One electrode is placed into the spinning solution and the other oppositely charged or neutral electrode attached to a conductive collector. If the charge build-up reaches an order of approximately 15 kV the charged compound droplet (poorly-conductive polymer solution) deforms into a conical structure called a Taylor cone. On further increasing the charge at the Taylor cone to some critical value (unique to each polymer system), the surface tension of the compound Taylor cone is broken and a core-shell jet of polymer solution ejects from the apex of the Taylor cone (Figure 3.9). This jet is linear for a small distance, then deviates in a course of violent whipping from bending instabilities brought about by repulsive charges existing along the jet length. The core-shell jet is stretched and solvent is evaporated and expelled, resulting in the thinning of the fiber. Ultimately dry (most solvent being removed) submicron fibers are collected in a simple collector design (water bath). The average collection time was 3 min. The mineral oil of the dry collected core-shell fibers is removed by immersion in octane. The aforementioned response was determined by measurement of core-shell diameters using scanning electron microscopy (SEM) and transmission electron microscopy (TEM).

The basic requirement for the formation of a stable Taylor cone by coaxial electrospinning includes:

A. Solution properties such as:

- Adequate shell viscosity ($15 \geq \eta > 4$ Pa.s (at δ 36 1/s))
- Adequate boiling point of the solvent (bp $\geq 100\ ^{o}C$)
- A conductive spinning solution ($2 \leq k \leq 5$ μS/cm)

B. Processing parameters such as

- Suitable core and shell feed rate combination
- Suitable electrode distance (spinning distance)

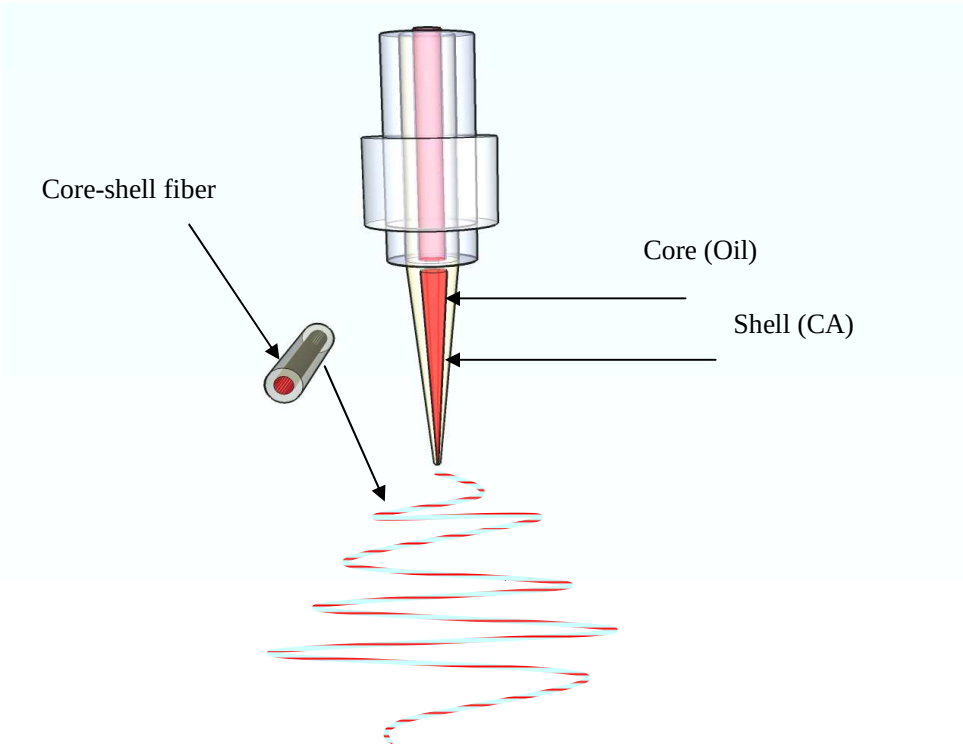

Figure 3.9: Schematic diagram of a co-electrospinning jet.

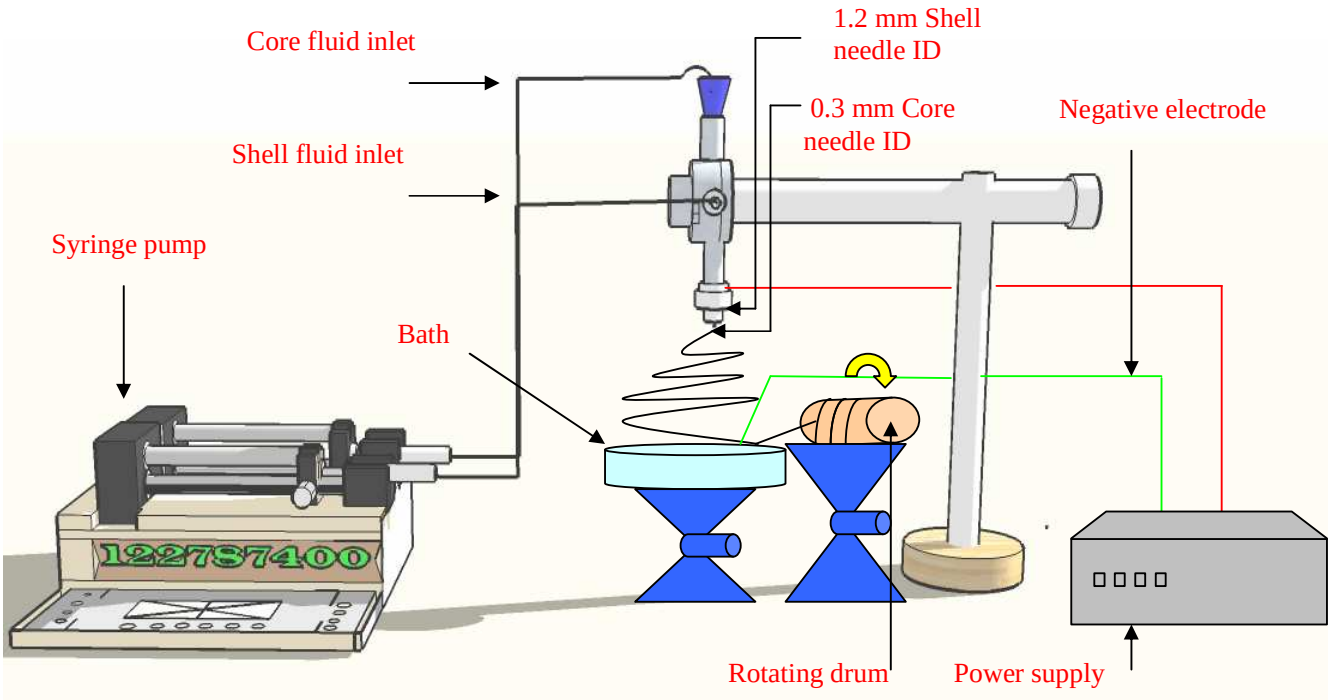

Figure 3.10: Schematic of co-electrospinning setup used.

3.5.3 Fiber alignment

Many different methods have been considered for fiber alignment [10, 51, 63-68]. Among them is the technique known as fiber collection using a water bath [68]. The technique involves a simple setup and exhibits a very high degree of fiber alignment. In this technique, electrospinning is carried out over the top of the water bath (Figure 3.11) in which the electrospun fibers are continuously deposited on the surface of the water. The web is elongated and alignment of the fibers takes place in the drawing direction. This technique has three important features:

- higher feed rate, to deliver sufficient fibers on the surface of the water so that the resultant fibers have sufficient strength
- low speed motor to draw the electrospun fibers from over the surface of the water to a small rotating drum (fiber collection speed is relatively slow)
- short critical distance, hence decreasing the distance between the needle and the collector owing to an increasing volume of the fibers depositing on the surface of the water

The advantage of having aligned fibers of a CA matrix is to allow their packing into a bundle form, in order to expose the hollow structure of the fibers.

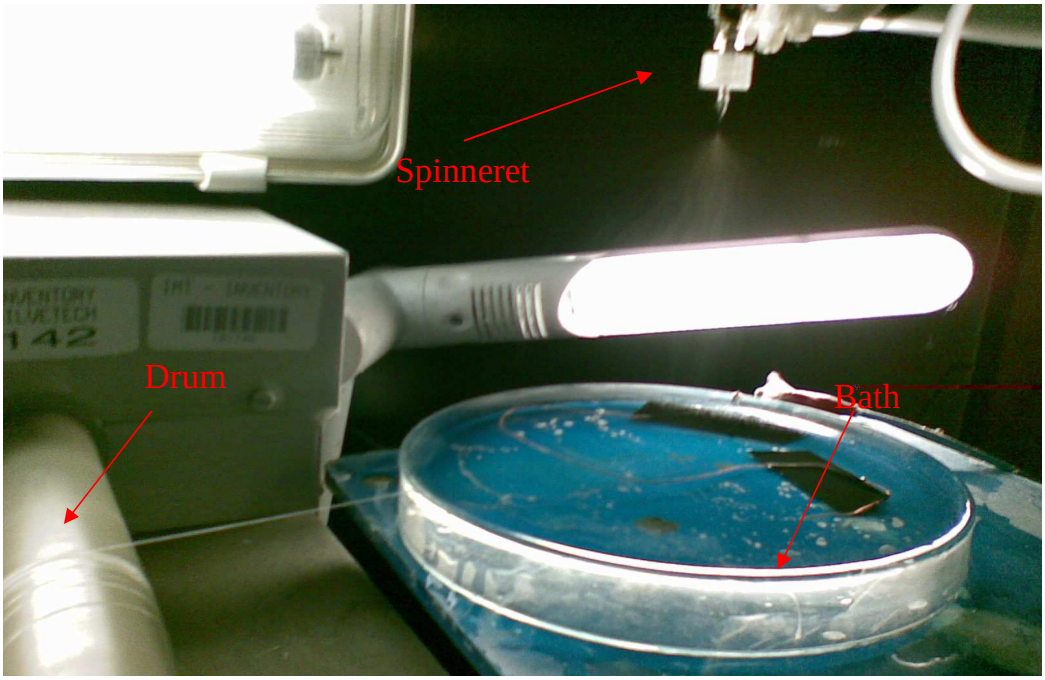

Figure 3.11: Fiber collections using a water bath.

In another technique [11], CA electrospun fibers were collected on a rotating wire drum (Figure 3.12). The biggest disadvantage of this method is that most of the fibers are not perfectly aligned while being collected on the rotating drum as they lose their alignment due to dispersion. Also, the aligned fibers are compacted on the wire rather than the whole drum, which makes it difficult to remove them.

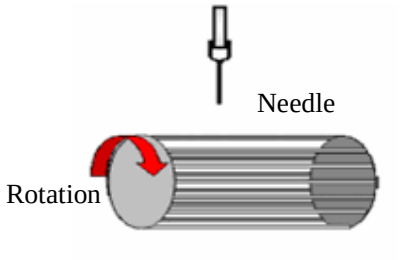

Figure 3.12: Schematic of a rotating wire drum collector [11].

In this study the continuous alignment of CA fibers was obtained by electrospinning onto a water reservoir collector (Figure 3.11). The technique is easy to use and the low fiber production rate makes it suitable for the laboratory-scale production electrospinning of nanofiber yarns.

3.5.4 Removal of fiber cores by solvent extraction

Removing the core is one of the key steps in producing hollow fibers. The solvent used to remove the core should meet the following criteria: it must dissolve the core but not dissolve the shell and it must not have any significant effect on the morphology of the formed fibers.

Octane is a straight-chain alkane and widely used in laboratories as a non-polar solvent which make it ideal to dissolve the mineral oil (non-polar). Octane is less flammable (high flash point), than the other shorter chain alkanes. Octane also has a good phase-separating ability and good extractability.

In this study octane used as the removing solvent to obtain hollow fibers. The core was extricated by immersing the electrospun fibers in octane over a period of 24 hr. Once the core had been completely removed the fibers were then left to dry at room

temperature. The obtained hollow fibers were analyzed for their morphology and structure by SEM and TEM analysis. Figure 3.13 shows schematic of the fabrication of hollow fibers.

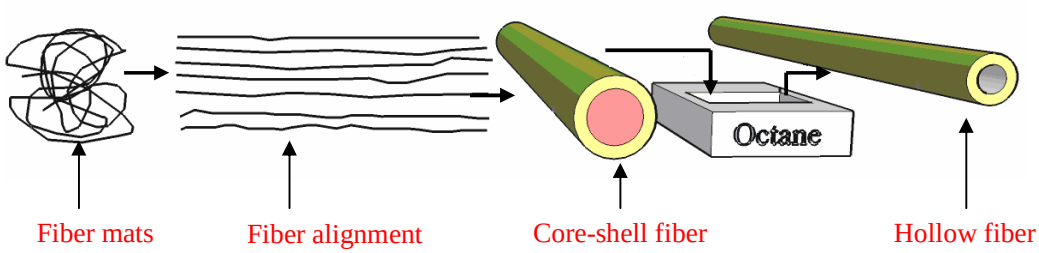

Figure 3.13: Schematic of the fabrication of CA hollow fibers.

3.6 Analytical procedures

3.6.1 Microtoming

A microtome is a mechanical device used to cut samples into clear, fine sections for microscopic inspection [69]. The blade is made of steel, glass or diamond. In this study a Reichert Ultracut-S microtome (Figure 3.14) with a steel blade and glass knife was used to slice sections for SEM and TEM analyses.

Figure 3.14: Photograph of microtome apparatus used in this study.

The obtained microtome cuts provided insufficient details about the morphology and structure of the fibers (results are shown in Appendix D). Therefore, this technique was not considered in further analysis.

3.6.2 Scanning electron microscopy

Scanning electron microscopy (SEM) is a technique that uses a beam of electrons instead of photons, and samples can be imaged at high magnifications. SEM measures the energy of X-rays that are generated by the atoms of the sample during interactions with the electron beam. The X-ray spectra formed are characteristic of the atoms that gave rise to them, revealing the chemical composition of the sample [70].

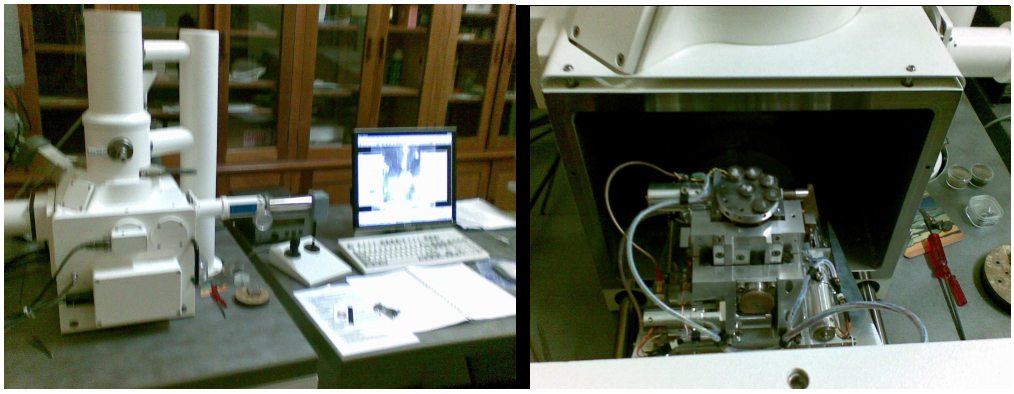

(A) (B)

Figure 3.15: (A) Photograph of Leo 1430 SE, (B) photograph of SEM chamber.

A scanning electron microscope (Figure 3.15) was used to characterize electrospun fibers. Characterization of these fibers included:

1. Examination of the morphology of the fibers
2. Examination of the cross section of the hollow fibers
3. Measurement of the inside and outside diameters of the hollow fibers

The fibers were frozen in liquid nitrogen and cut into pieces about 3 mm long, ensuring that the microstructure remained intact and then carefully mounted on the top of the SEM tag. The samples were then coated with a single gold layer (1 min) and then loaded into the chamber of the SEM apparatus. All images were recorded between 190x and 2000x magnification, at 7 kV voltage.

3.6.3 Transmission electron microscopy

Unlike SEM, TEM has the ability to determine the internal structure of materials by using an electron beam that passes through the very thin sample and the image forms on a fluorescent screen. A JEOL CX200 TEM apparatus was used to characterise the core-shell structure of the fibers and provides evidence of the existence of the core. The fibers were carefully mounted on the top of the TEM grid (Figure 3.16) and loaded in the chamber of the TEM apparatus.

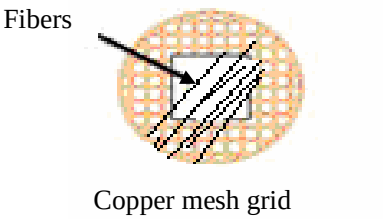

Figure 3.16: TEM grid.

3.6.4 Fiber diameter measurement via image analysis

Before commencing with image analysis the contrast of each image was optimized in an attempt to identify the cross-sections of the electrospun hollow fibers. The images were analyzed by measuring the fiber diameters (ID and OD). This was done using SEM Image Studio software (version 1.10). The fibers were analyzed manually, by measuring the diameters of each fiber, from an individual image. Two images of each sample were analyzed. About 20-50 fibers in each photograph were randomly selected for the measurement. The analysis was done by first setting the scale and measuring manually. The measurements were made by dragging the cursor towards the entire width of the diameter. The results of the measurements were then exported to a Microsoft Excel sheet and the average fiber diameters measured. The calculated value of the average standard deviation (15) suggested low deviation associated with the measurements (see Appendix A).

Chapter 4

Results of initial investigation

4.1 Introduction

The objective of the initial investigation is to study the effect of the process and system electrospinning parameters on the electrospun fibers, in order to determine the more important parameters that influence the formation of CA hollow fibers. The investigation includes the consideration of the behaviour of the coaxial jet, the stability of the electrospinning process, and the morphology and structure of the electrospun fiber.

4.2 System validation

In order to confirm that the coaxial electrospinning design (Figure 4.1) was in functioning order and capable of electrospinning, a series of CA/oil control solutions were spun and then observed using transmission electron microscopy (TEM) and scanning electron microscopy (SEM).

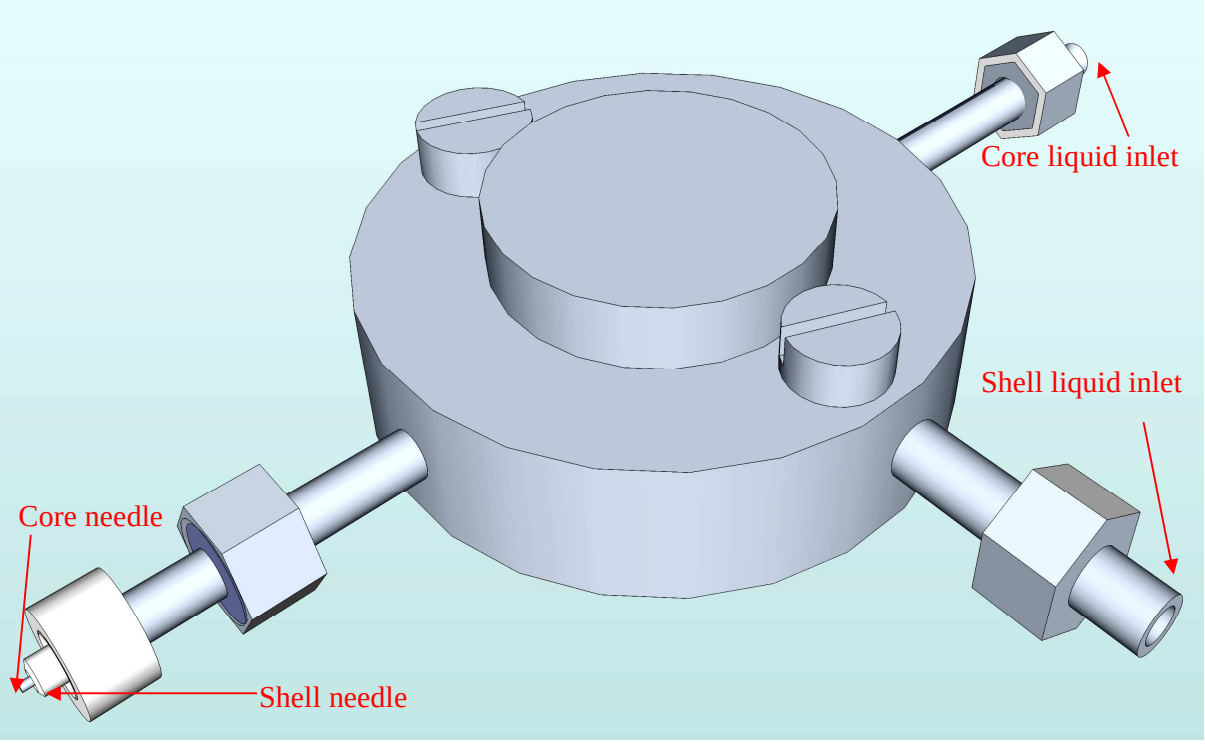

Figure 4.1: Schematic of coaxial spinneret developed in this study.

The following TEM and SEM images (Figures 4.2 and 4.3) verified the capability of this new coaxial electrospinning design to electrospin solutions that meet the essential requirements of electrospun core-shell fibers.

Hollow fibers with an average inside and outside diameter of approximately 459 and 1266 nm, respectively, were successfully electrospun using the new co-electrospinning design.

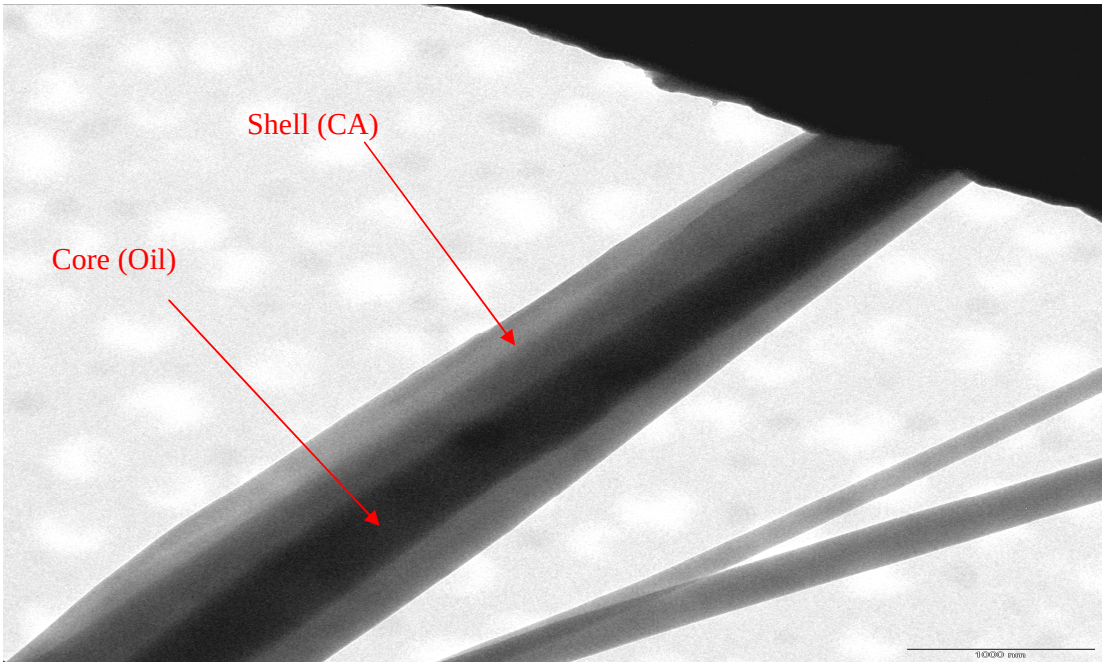

(A)

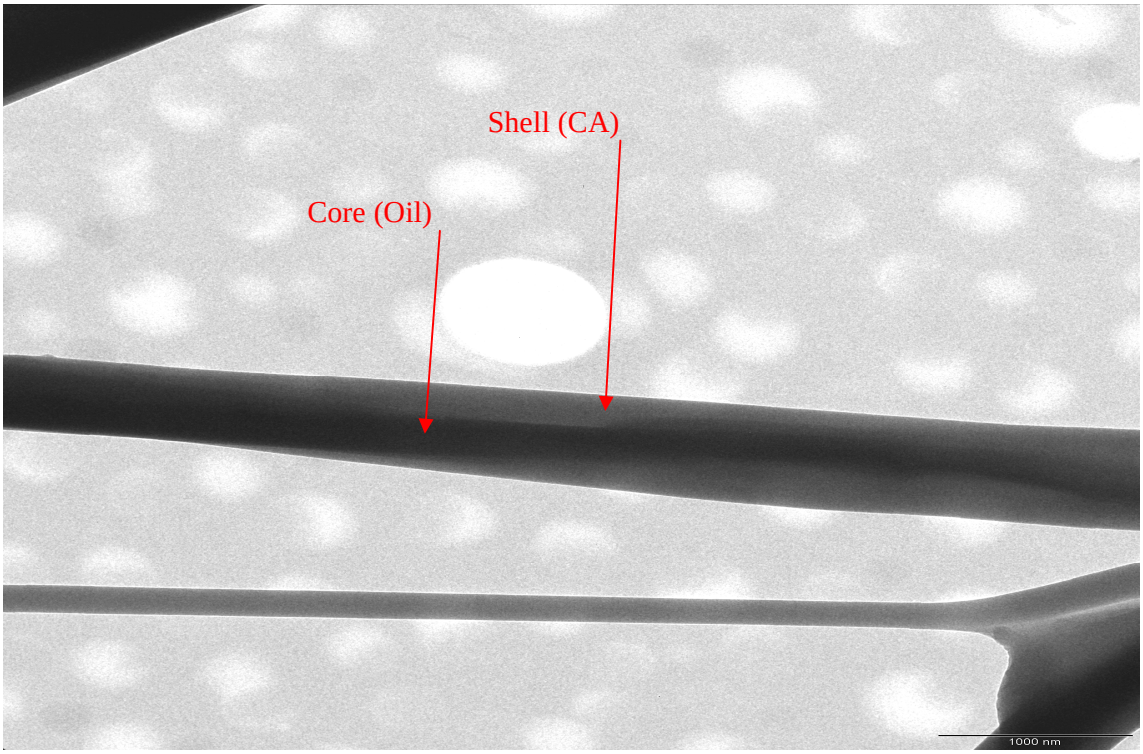

(B)

Figure 4.2: (A) and (B) TEM images of electrospun core-shell fibers of CA.

(A)

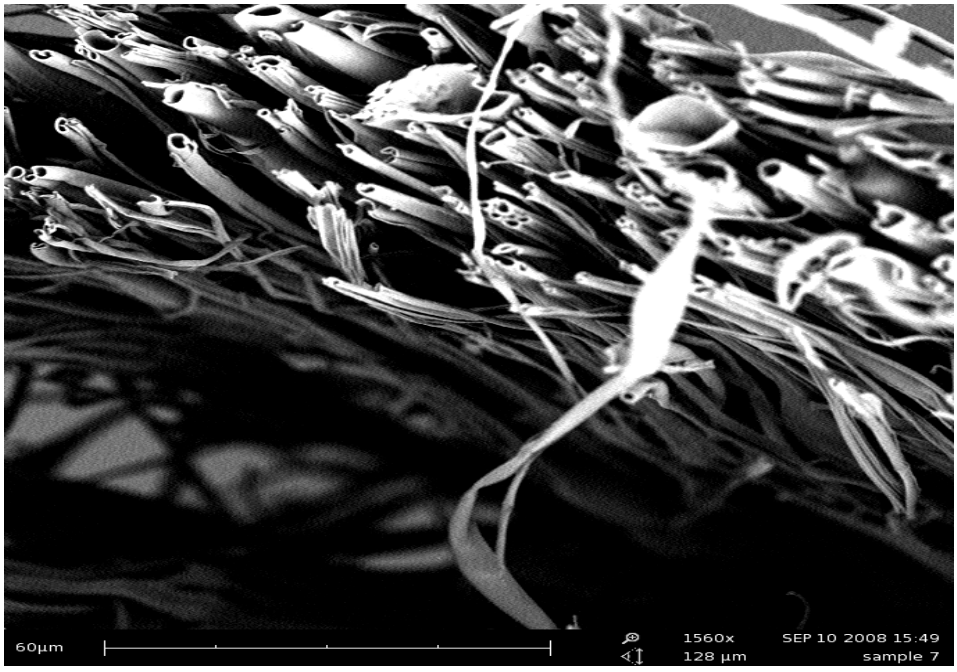

(B)

Figure 4.3: (A) and (B) SEM images of electrospun hollow fibers of CA prepared by co-electrospinning.

4.3 Co-electrospinning

In order to determine the optimum co-electrospinning process, the spinability of the solution and the morphology, i.e. fiber diameter and uniformity of the electrospun hollow fibers, were studied. In order to estimate the spinability of the spinning solutions, a common visual classification system was used [34, 36, 71]. The behaviour of the co-electrospinning jet was classified as either dripping or whipping electrospinning. (The visual classification of the spinning solution was carried out during the electrospinning process for different spinning solution concentrations and core-shell feed rate values). Figures 4.4 and 4.5 show the behaviour of the co-electrospinning jet in terms of the spinning solution concentration, shell feed rate and core feed rate. Dripping was observed during the electrospinning process at different shell feed rate values. As the shell feed rate decreased a stable Taylor cone was formed, but it only produced drops on the collection plate. This type of dripping was observed below a shell feed rate and spinning solution concentration of 1 ml/hr and 11 wt % respectively.
The linear velocity of both fluids (core and shell) was calculated and the values are found to be 2 and 0.7 mm/s for the core and the shell respectively (see Appendix E).

Co-electrospinning produces CA nanofibers during the whipping phase. Both Figures 4.4 and 4.5 show that the highest value of whipping jet increases as the spinning solution concentration increases (the ability of a polymer solution to be electrospun is governed by the number and size of polymer chains in the spinning solution; essentially, the chain entanglements should form continuous fibers when a high polymer concentration is introduced to the spinneret (possibly in a limited range)). A stable whipping jet was observed when the shell feed rate and core feed rate were 3 and 0.5 ml/hr, respectively. The spinning solution generally required a shell feed rate of about 5 ml/hr and a core feed rate of about 0.5 ml/hr to achieve whipping. If the shell solution feed rate is higher than the optimum range then the excess solution will drip out. When the core solution feed rate is too high no core-shell structured fibers are formed.

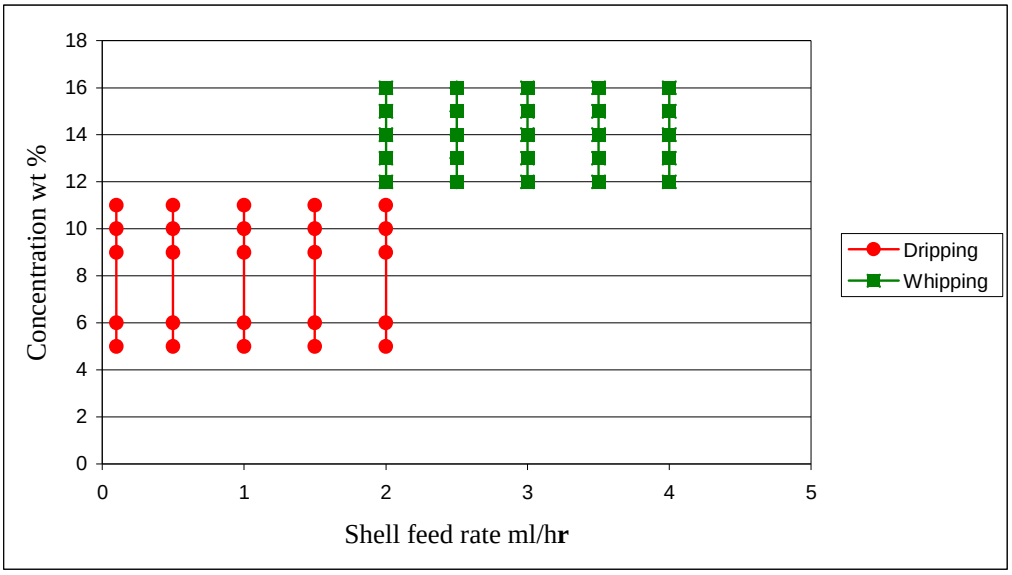

Figure 4.4: Co-electrospinning visual classification of CA spinning solution in terms of spinning solution concentration and shell feed rate (2 mm/min shell linear velocity at shell feed rate of 3 ml/hr).

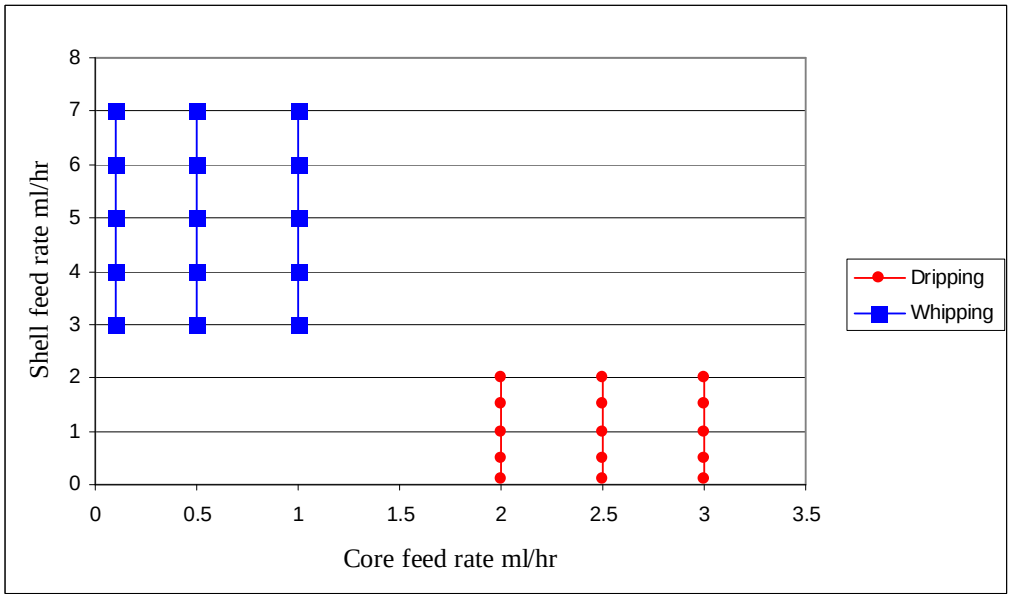

Figure 4.5: Co-electrospinning visual classification of CA spinning solution in terms of core and shell feed rates (2 and 0.7 mm/min the core and shell linear velocity at 0.5 and 3 ml/hr core and shell feed rate respectively).

4.4 Effects of electrospinning system parameters

Many system parameters can influence the transformation of polymer solutions into nanofibers through electrospinning. These parameters include polymer concentration, type of solvent, solvent ratio, solution conductivity and solution surface tension.

4.4.1 Effect of polymer concentration

The ability of a polymer solution to be electrospun is governed by the number and size of polymer chains in the spinning solution; essentially, the chain entanglements should form continuous fibers when an electric field is introduced to the polymer solution. A polymer solution with a concentration (and viscosity) that is too high or low cannot be successfully electrospun. The viscosity shear measurements for CA solutions showed that a viscosity of the solution in range of 4-15 Pa.s is required for a CA solution to electrospin.

The fiber formation is dependent on the polymer concentration, which has a significant effect on the morphology, quality and diameter of the electrospun fibers. A number of experiments were carried out to determine the lower limit of CA polymer concentration. It was found that fibers with many beads formed when a CA concentration of 11 wt % was used (see Figure 4.6). At this polymer concentration the molecular chain entanglement in the polymer solution was insufficient, and hence the lower limit on the concentration of the solution was accepted to be 12 wt %. In order to determine the upper limit of the polymer concentration, the concentration of CA was varied from 12 to 15 wt % while holding the other parameters constant, including the core and shell feed rate, solvent ratio, voltage and spinning distance. It was found that at a CA concentration of 15 wt % it was difficult to form fibers due to block taking place at the tip of the capillary. The reason could be that the viscosity of the solution was too high, compared with that of solutions of concentrations of 11, and 12 wt %. At a concentration of 11 wt % the viscosity was too low ($\eta < 4$ Pa.s at shear rate of $\delta > 35$ 1/s), it was difficult to form a stable jet, and at concentration of 15 wt % the viscosity was slightly high ($\eta > 14$ Pa.s at shear rate of $\delta < 17$ 1/s), it was difficult to form fibers due to drying at the tip of the

needle. Hence, it was determined that the most suitable polymer concentration would be in the range of 12 to 14 wt %.

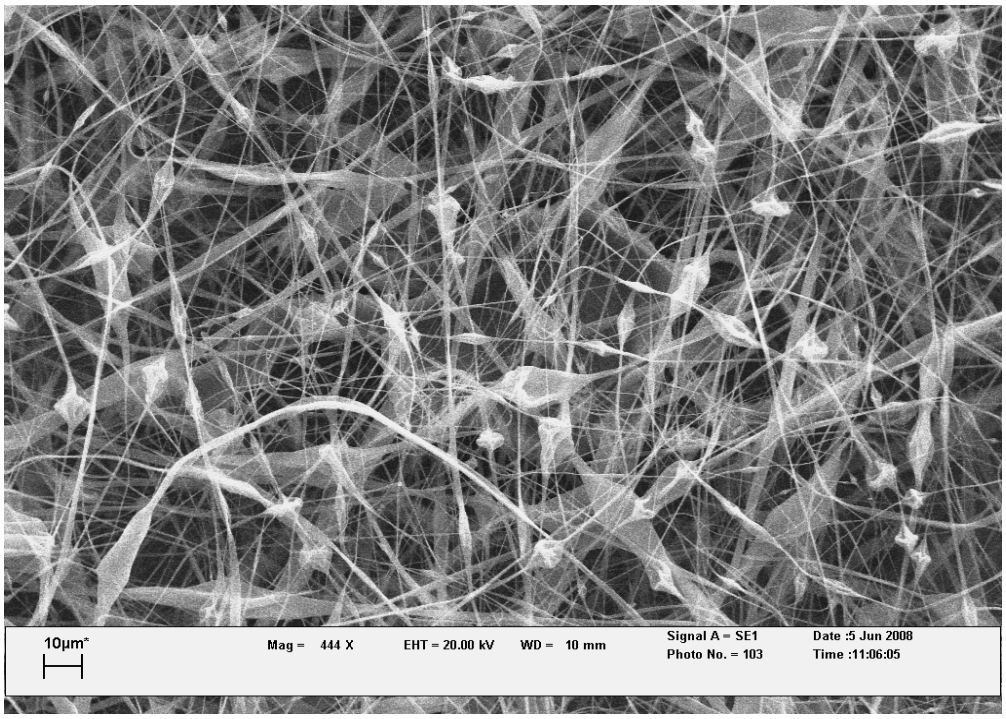

(A)

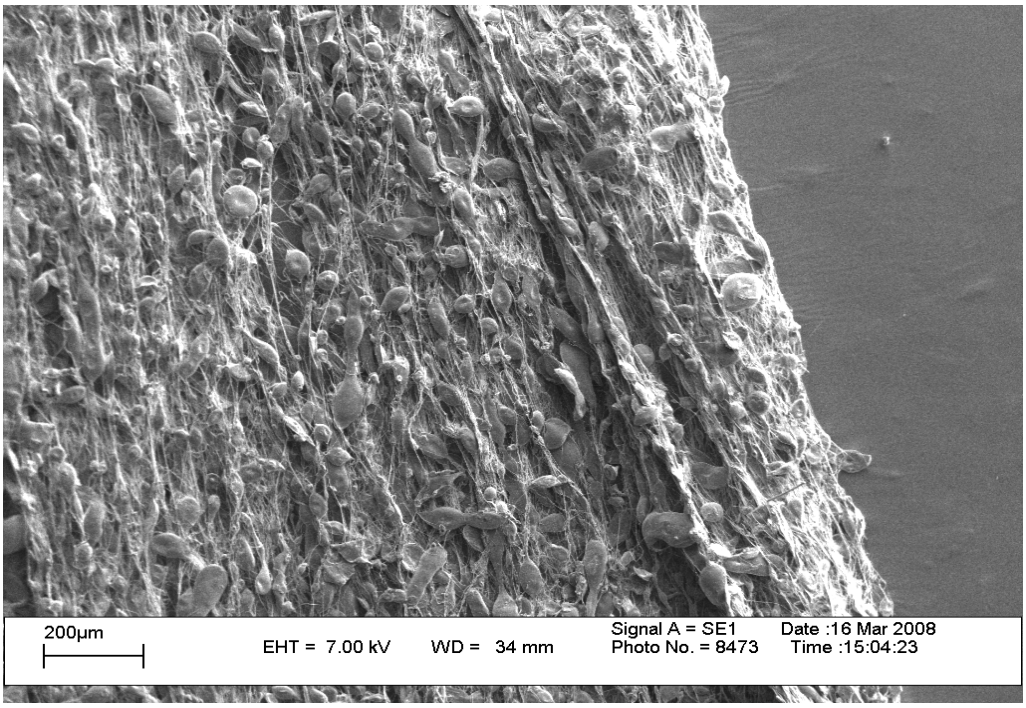

(B)

Figure 4.6: SEM micrographs of CA nanofibers electrospun from an 11 wt % CA solution: (A) before the alignment and (B) after the alignment, showing the formation of beads.

When evaluating the morphology of the fibers it is the average fiber diameter that is the most important factor to consider.

General theory states that the polymer solution with a high polymer concentration, will have a high viscosity, and hence a polymer solution with a high concentration, will yield fibers with a large diameter [71]. SEM images of fibers spun for polymer solutions with different concentration (12 wt % and 14 wt %) are shown in Figures 4.7 and 4.8. The diameters of the hollow fibers measured using SEM image studio software were the following. Fibers spun from a 12 wt % CA solution had ID 417 nm and OD 1132 nm, and from a 14 wt % solution ID 1158 nm and OD 2881 nm. This indicates quantitatively that the inner and outer diameters increase with increasing polymer concentrations.

Figure 4.7: SEM image of hollow fibers electrospun from a 12 wt % CA solution. Mag (877x)

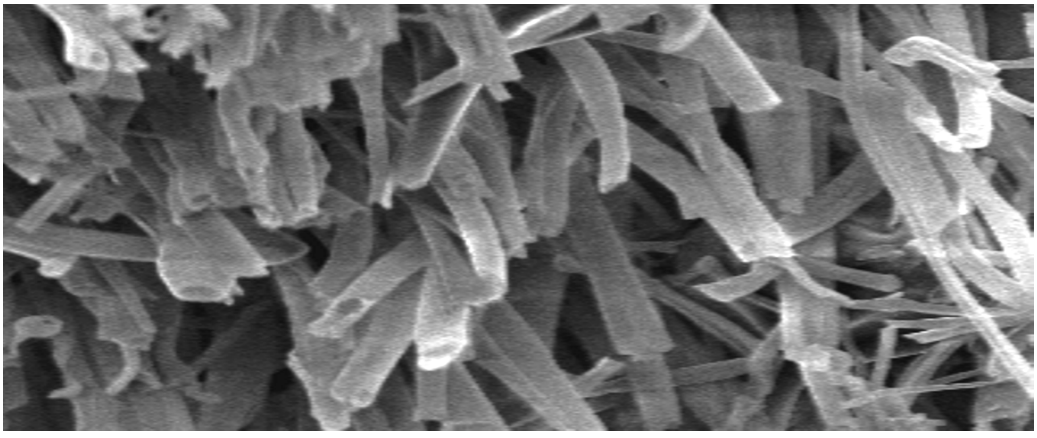

Figure 4.8: SEM image of hollow fibers electrospun from a 14 wt % CA solutions. Mag (1000x)

4.4.2 Effect of type of solvent

Various solutions and solvent systems were studied, including: acetone, dimethylacetamide (DMAc), dioxane, methanol, acetic acid, ethanol, and water and ethylene chloride. The experimental procedures followed for the preparation of the solutions are carefully explained in Appendix A. Fibers spun from polymer solutions, in the selected solvents, were characterized by studying their fiber morphology.

The fiber-formation productivity (Table 4-1) was determined. Some fibers with beads were obtained from solutions of CA in acetone:DMAc with different concentrations (10, 12, 14 and 16 wt %) as shown in Figure 4.9. Cellulose acetate in the following solvent systems did not yield fibers: acetone:methanol; acetone:ethanol; ethanol:methanol; and acetone. When ethylene chloride:ethanol; acetic acid:water or dioxane:acetone:methanol:maleic acid were used as solvents the jet was formed but there was a tendency to electorspray rather than electrospin, and the spinning solution often blocked the tip of the spinneret. This is probably due to the low boiling point of the main solvent, resulting in rapid evaporation of the solvent during the electrospinning process. The physical properties of the solvents used such as density and boiling point, are tabulated in the Appendix A, Table A2.

Table 4-1: Effect of solvent and solution concentration on electrospun CA fibers (Electrospinning conditions: CA feed rate 5 ml/hr, spinning distance 11 cm and Voltage 15 kV.)

Solvent	Solvent ratio (v/v)	CA (wt %)	Observation
Acetone:DMAc	1:1, 2:1, 3:1	10;12;15; 17	Fibers and beads
Acetone:methanol	1:1, 2:1	12	No Electrospinning
Acetone:ethanol	2:1	12	No Electrospinning
Acetone:methanol:ethanol	2:1:1	12	No Electrospinning
Ethylene chloride:ethanol	80:20	10	Few fibers
Acetic acid:water	80:20	16	Few fibers
Dioxane:acetone:methanol: maleic acid	45.1, 28.7, 7.2, 2.4	16.4	Thick fibers
Acetone:dioxane	2:1	12;15	Fibers membrane

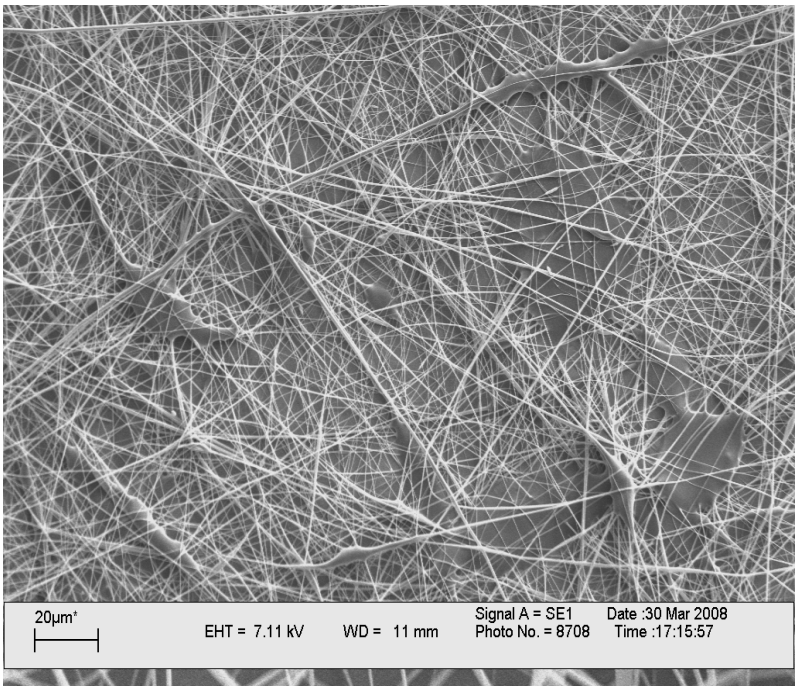

(A)

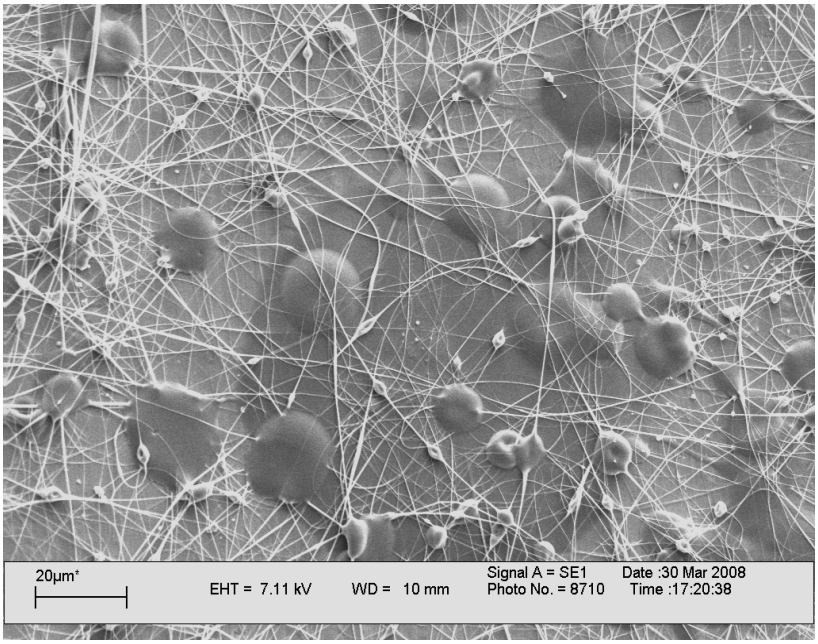

(B)

Figure 4.9: SEM images of electrospun fibers fabricated from solutions of CA in acetone:DMAc (2:1), electrospun onto aluminium foil: (A) 14 wt % CA , (B) 12 wt % CA.

When acetone:dioxane (2:1) was used as solvent the jets appeared to be continuous, forming clean fibers without beads, as shown in Figure 4.10. The 2:1 acetone:dioxane was considered to be the most suitable solvent system because it allowed the continuous electrospinning of CA solutions and produced uniform fibers.

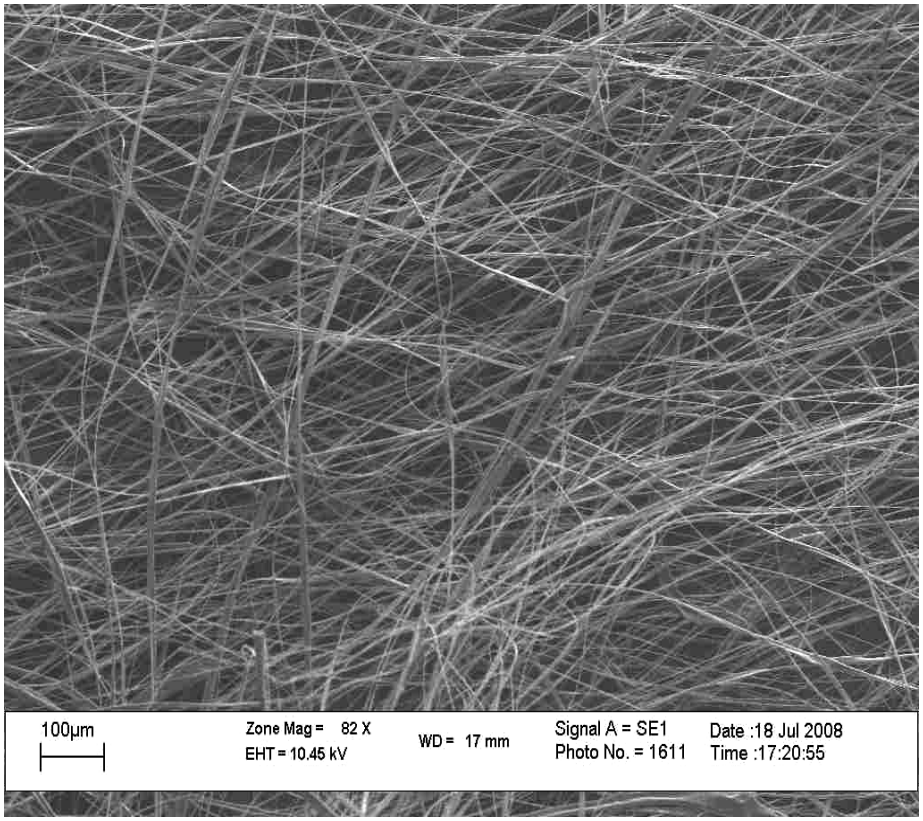

Figure 4.10: SEM image of electrospun fiber fabricated from 14 wt % CA in acetone:dioxane (2:1), electrospun onto wire drum.

4.4.3 Effect of solvent ratio

The effect of the solvent ratio in a solvent mixture on electrospun CA fiber diameter was investigated for single electrospinning. When acetone alone was used as a solvent the resulting CA solution was difficult to electrospin due to clogging of the spinning solution at the tip of the needle. This occurred because of the low boiling point of the acetone (56 ^{o}C) which resulted in rapid evaporation of the spinning

solution. Tungprapa et al. [59] found that blocking of the spinning solution at the tip of the nozzle can be reduced by addition of a co-solvent; it improved the electro-spinnability of a CA solution. Successes achieved with using a co-solvent or mixture of solvents could be ascribed to the higher boiling points and dielectric constants of the co-solvent.

Acetone was then mixed with dioxane in different ratios, i.e. 1:1, 2:1, 3:1 and 5:1 (v/v) acetone:dioxane and used, to dissolve CA powder to prepare spinning solutions of different CA concentrations (11, 12, and 14 wt %). Electrospinning of all these mixed solutions resulted in the continuous electrospinning of CA solutions and afforded fibers in different morphologies. Table 4.2 shows the experimental conditions and the results of the experiments. The different solvent ratios used had practically no effect on the fiber diameters of electrospun CA fibers.

Table 4-2: Effect of acetone:dioxane ratios on electrospun CA fibers

(Electrospinning conditions: Feed rate 5 ml/hr, spinning distance 11 cm and voltage 15 kV.)

Solvent	Ratio (v/v)	CA (wt %)	Observation	Time of continuous electrospinning
Acetone	–	11;12;14	None	0 s
Acetone:dioxane	1:1	11;12;14	Few fibers	< 60 s
Acetone:dioxane	2:1	11;12;14	Fibers membrane	> 15 min
Acetone:dioxane	3:1	11;12;14	Few fibers	< 60 s
Acetone:dioxane	5:1	11;12;14	Few fibers	< 60 s

4.4.4 Effect of Conductivity

The spinning solution is held in a droplet shape by surface tension. An electrical field is created when the high voltage is supplied to a needle immersed in the spinning solution. A charge is induced on the surface of the droplet. When the electric field increases charges on the surface of the droplet increase until the spherical drop distorts into a Taylor cone. When the charges that are carried by the solution increase, the stretching of the solution will also increase and result in the formation of smooth fibers. On the other hand, bead formation will occur if the solution is not fully stretched.

A spinning solution with low conductivity causes the diameter of the as-spun fibers to decrease. An increase in conductivity results in increased electrostatic forces on the jet and causes the jet to travel with greater velocity closer to the collector. This results in a decrease in the total flying path of the jet, which will result in a decrease in the chance of the jet being stretched by the coulombic stress, and therefore fibers with larger fiber diameters result [15,72]. Table 4.3 shows the conductivity of CA solutions for four different concentrations.

Table 4-3: Conductivity of CA solutions in 2:1 (v/v) acetone:dioxane

Concentration (wt %)	Conductivity (μS/cm) at 20 °C
11	2
12	3
14	2
15	3

4.4.5 Effect of surface tension

Surface tension is a property of the surface of a liquid that makes it act as an elastic sheet, and it reduces the surface area per unit mass of a fluid. The surface tension of a solution is directly influenced by the concentration of solvent molecules [16, 21]: at a high concentration of solvent molecules, the molecules take on a spherical shape as a result of the effect of the surface tension, which leads to the formation of beaded fibers (Figure 4.11). On the other hand, when the viscosity of the fluid is high there is greater interaction between solvent and polymer molecules. This interaction effect leads the solution to be stretched by the electric field, when the force of the electric field overcomes the surface tension the solvent molecule will spread over the entangled molecules and therefore reduce the tendency for the solvent molecules to coalesce under the effect of surface tension (which leads to the formation of beads). As both the surface tension and polymer concentration increase formation of non-beaded fibers is favoured. The resulting non-beaded and smooth fibers can be attributed to a combination of both increased concentration and surface tension.

Table 4-4 shows the surface tension of CA solutions for four different concentrations.

Table 4-4: Surface tension of CA solutions in 2:1 (v/v) acetone:dioxane

Concentration (wt %)	Surface tension (N/m)
11	28.2
12	28.8
13	29.1
14	30.5

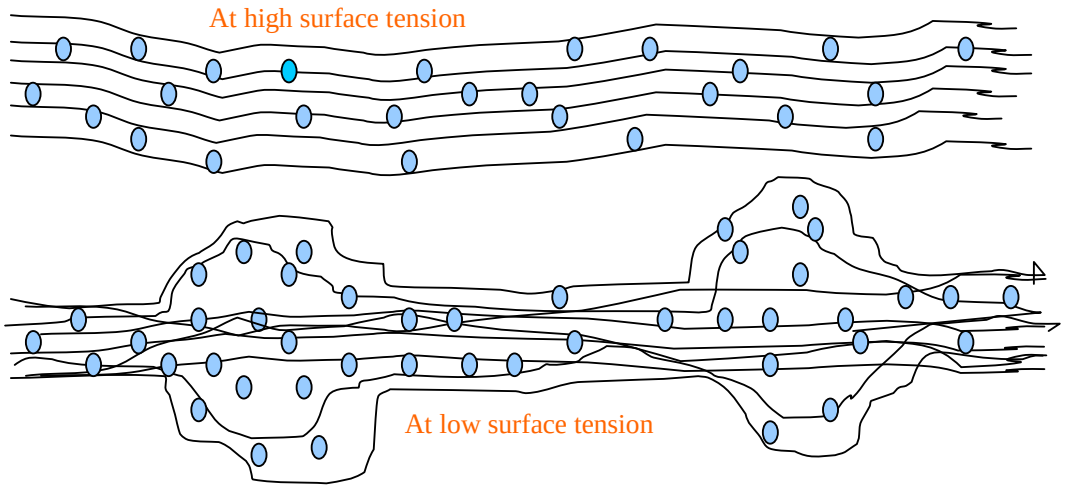

Figure 4.11: Effect of surface tension on uniformity of fibers (smooth and beaded fibers, respectively**).**

4.5 Beads formation

In this research the solvent type and solution concentration were found to have a significant influence on the morphology of the fibers and formation of beads. The percentage of beads was found to increase in the fibers at low solution concentration (Figure 4.12). The type of solvent and the ratio of solvents were also found to be responsible for the formation of beads. Fibers produced from a solution of CA in acetone:DMAc with different ratios (1:1, 2:1 and 5:1) formed beads on the fibers at different CA concentrations (11-16 wt %). The influence of the solvent on bead

formation was studied by Wannatong et al. [14] in the electrospinning of a polystyrene (PS) solution. They found that a large difference between the values of the solubility parameter of the polymer and a solvent induces retraction of the polymer molecules due to the poor fundamental interaction between the polymer and the solvent molecules, causing bead formation in the resulting fibers. Surface tension and polymer solution viscosity are other key parameters that affect the formation of beads on fibers.

The spinning solution is held by the surface tension effect, which acts to make the surface area of the droplet small. When the electrical field increases the charge on the surface of the droplet also increases to allow for an increasing surface area, which resists the bead formation [73]. Figure 4.12 shows the morphology of beaded CA fibers.

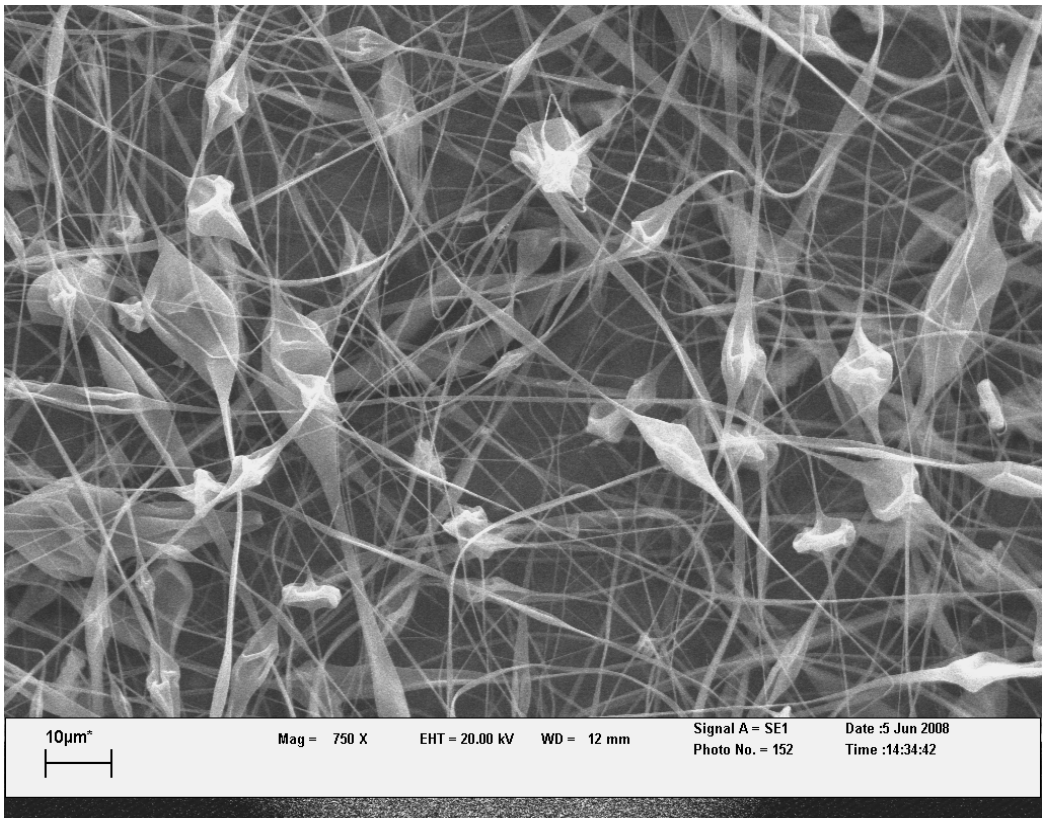

Figure 4.12: The morphology of beaded fibers fabricated from a 11 wt % CA solution in acetone:dioxane (2:1), electrospun onto aluminium foil.

4.6 Effect of electrospinning process parameters

Effects of selected processing parameters on the morphology, i.e. fiber diameter and its uniformity, of electrospun fibers were studied. These parameters include, core and shell feed rate, spinning distance, spinneret diameter and voltage.

4.6.1 Effect of core and shell feed rate

Both the core and the shell solutions were introduced at independent feed rates to the core and shell needles respectively. Appropriate flow rates are necessary to control the amount of whipping and to reliably produce nanofibers.

Visual examination of fibers for the effect of the core and shell feed rates on the behaviour of the electrospinning jet revealed that when the shell solution feed rate is lower than the optimum range the Taylor cone can be broken. On the other hand, if the shell solution feed rate is higher than the optimum range then the excess solution will drip out. When the core solution feed rate is too high no core-shell structured fibers are formed. Zhang et al. [74] explained that such behaviour can occur when the feed rate of the shell solution is too low to wrap the core solution.

The feed rate of polymer solution acts as the most important factor in the process of electrospinning by maintaining the stability of the Taylor cone. Controlling the solution feed rate is essential. Evidence shows that in coaxial electrospinning there is an optimum range of feeding rates for successful electrospinning in order to maintain a stable coaxial jet [74]. The optimum feed rate range is from 0.5 to 1 ml/hr for the shell solution and 1 to 3 ml/hr for the core (2 and 0.7 mm/min the core and shell liner velocity, respectively). Feed rates above or below these values lead to an unstable jet and the formation of non-uniform fibers (Table 4-5).

Table 4-5: Effect of core and shell feed rate on electrospun CA fibers

(Electrospinning conditions: Solvent ratio 2:1 acetone:dioxane, spinning distances 11 cm and Voltage 15 kV.)

Core feed rate (ml/hr)	Shell feed rate (ml/hr)	CA (wt %)	Observation	Observation
				Whipping/dripping
0.5 to 2	1 to 10	11	No Electrospinning	Dripping
0.5 to 1	1 to 3	12	Fine fibers	Whipping
1 to 4	4 to 10	12	Few fibers	Dripping
0.5 to 1	1 to 3	14	Thick fibers	Whipping
1 to 4	3 to 10	14	Few fibers	Dripping

Figure 4.13 shows SEM image of 14 wt% CA hollow fibers fabricated using different shell feed rates, that there is dissimilarity in the fiber diameters between the two images. The low shell feed rate yields smaller diameter fibers.

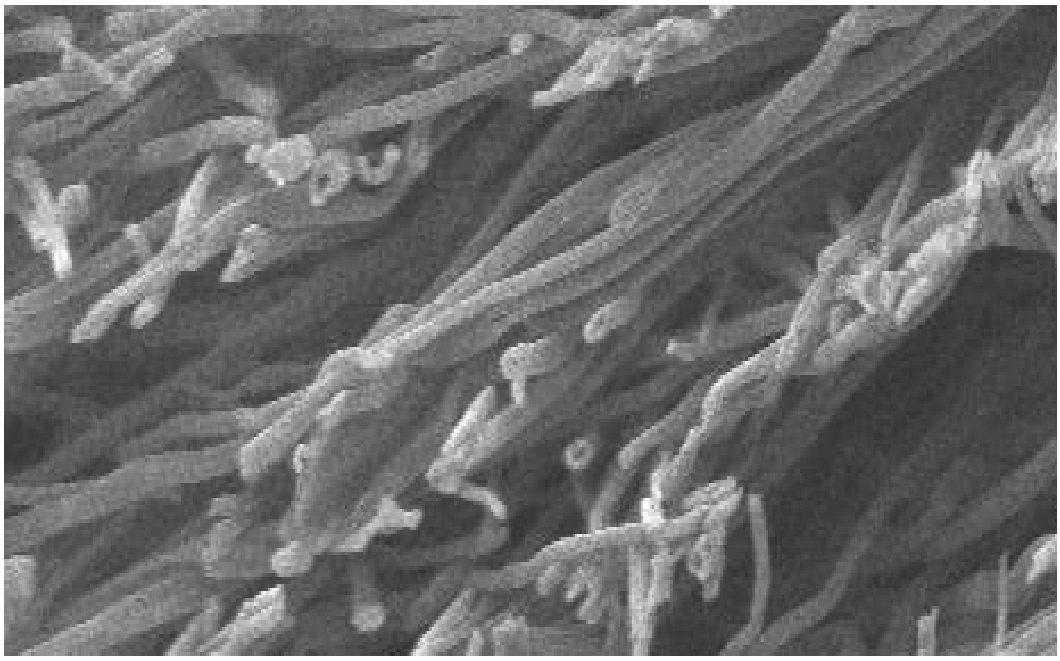

(A)

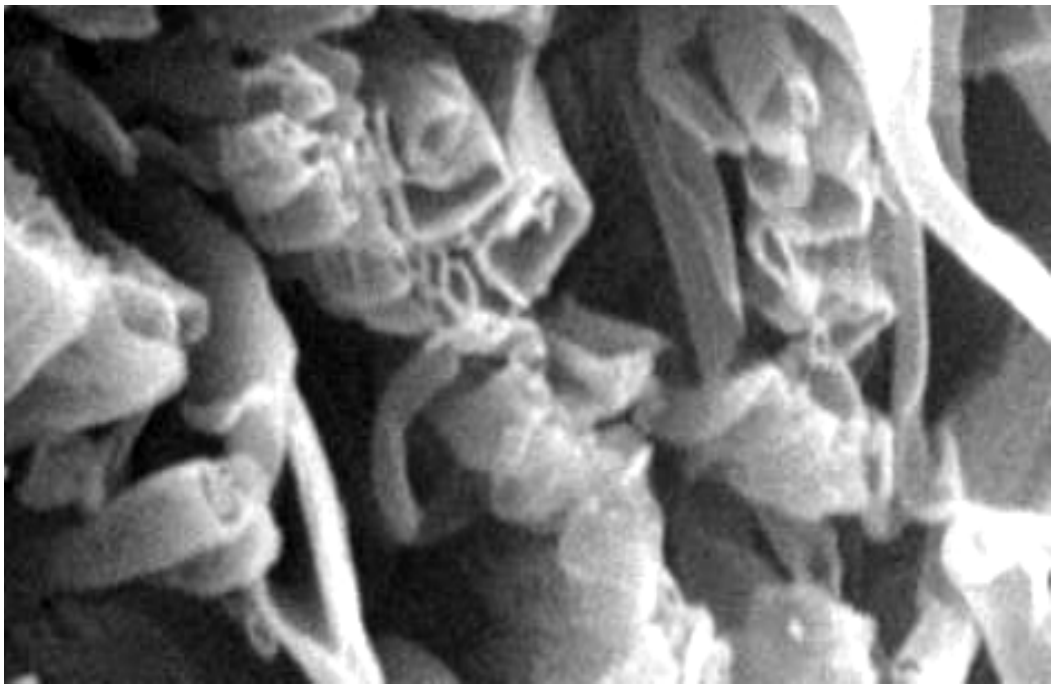

(B)

Figure 4.13: SEM images of 14 wt % CA hollow fibers fabricated using different shell feed rates. (A) 1 ml/hr Mag (1111x), (B) 3 ml/hr Mag (1000x)
(Electrospinning parameters: core feed rate 1 ml/hr, spinning distance 8 cm.)

4.6.2 Effect of spinning distance

The distance between the spinneret and collector is another factor that can affect the fabrication of hollow fibers and the number of collected fibers. Due to the nature of the collector used the spinning distance has a very limited range of variability. It was found that at larger spinning distances fewer fibers were deposited on the collector and the jet was unstable. However, at closer spinning distances the solvents did not have enough time to evaporate. These simple laboratory observations indicated that the distance between the spinneret and the collector could be varied from 8 to 11 cm.

Figures 4.14 and 4.15 show SEM images of fibers produced using 14 wt % CA in acetone;dioxane (2:1), 0.5 ml/hr core feed rate, 3 ml/hr shell feed rate and a spinning distance of 11 cm and 8 cm respectively. The hollow fibers produced at 8 cm spinning distance appear more uniform and have a neat hollow structure compared with the fibers produced at 11 cm spinning distance.

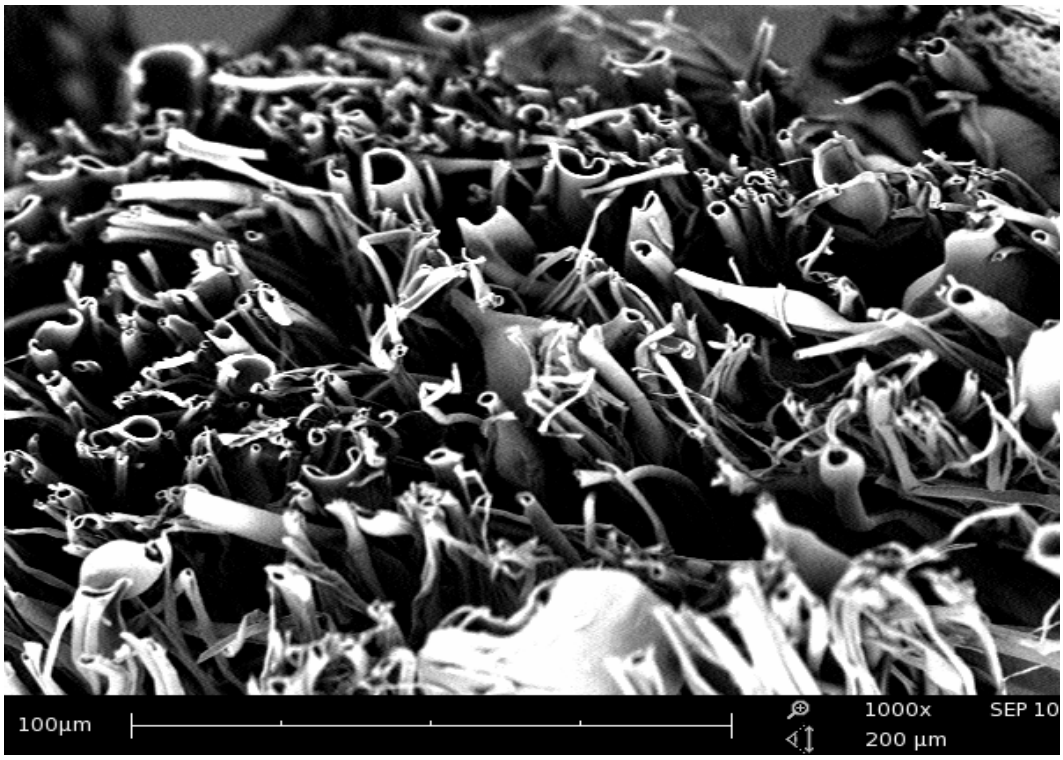

Figure 4.14: SEM image of electrospun hollow fibers produced using a CA polymer concentration of 14 wt % at a distance of 11 cm.

Figure 4.15: SEM image of electrospun hollow fibers produced using a CA polymer concentration of 14 wt % at a distance of 8 cm.

4.6.3 Effect of spinneret diameter

In order to study the effect of the spinneret diameter on electrospinning three different shell spinneret diameters were tested: large, medium, and small (2, 1.2 and 0.8 mm). It was found that the shell solution dripped out when a larger inner diameter was used. The reason is obviously the larger the inner core spinneret diameter the easier the flow. When a smaller inner diameter was used the shell spinneret diameter was too small for the core spinneret to be fitted in. Therefore, the medium inner diameter (1.2 mm) was found to be the most suitable inner diameter for the shell spinneret. The core spinneret inner diameter was fixed at 0.3 mm for it to be able to fit straight through the shell spinneret and create a coaxial spinneret design (see Appendix E, Figure E1).

4.6.4 Effect of voltage

A series of experiments was carried out to study the effect of voltage on the electrospun fibers. The voltage was varied from 10 to 20 kV while holding all other parameters constant. Results are tabulated in Table 4-6. This simple laboratory observation clearly indicated that varying the voltage from 15 kV resulted in an unstable electrospinning jet (see Figure 4.16). Hence the voltage was maintained at a value of 15 kV, to maintain Taylor cone in an equilibrium.

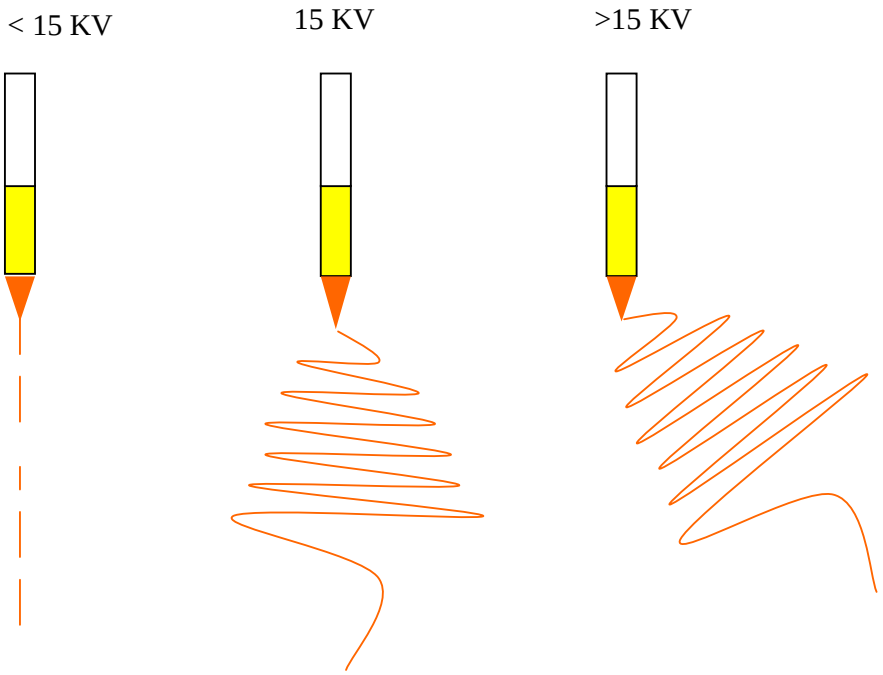

Figure 4.16: Schematic of the effect of the voltage on an electrospinning jet.

Table 4-6: Effect of the voltage on an electrospinning jet

(Electrospinning conditions: CA concentration 14 wt %, Solvent ratio 2:1 acetone:dioxane, core and shell feed rate 0.5, 2 ml/hr respectively and spinning distances 11 cm.)

Voltage (kV)	Jet behaviour	
	Observation	Appearance
5	Dripping	Not stable
10	Dripping	Not stable
15	Whipping	Stable
20	Whipping	Not stable
25	Whipping	Not stable

4.7 Effect of ambient conditions

4.7.1 Effect of humidity

Relative humidity has a slight effect on the morphology of the electrospun fibers. Fibers electrospun at 30 % relative humidity are smooth, non-porous fibers. Above 50 % relative humidity, there is a visible difference in the surface morphology of the fibers [30].

In this study it was found that fibers electrospun at high relative humidity (70%) had porous surfaces (Figure 4.17), whereas fibers electrospun at lower relative humidity (40%) had smooth, non-porous surfaces. It can be concluded that increasing the humidity causes an increase in the number of pores on the surface of the fibers.

Srinivasarao et al. [75] established the possibility that micropores in fibers can form due to a mechanism similar to the mechanism of air bubble formation in a polymer film. Li and Xia [76] later provided illustrative studies for the mechanism of micropore formation. They demonstrated that cooling resulted from the evaporation of solvent, causing the moisture in air to nucleate and water droplets to grow, and which finally evaporate and leave behind a film full of ordered pores.

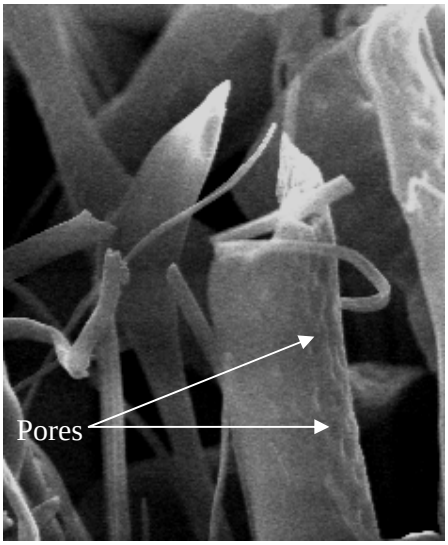

Figure 4.17: Effect of humidity (68 %) of a 15 wt % CA solution on the fiber morphology, Mag (487x).